Correlated Chained Gaussian Processes for Datasets with Multiple Annotators

J. Gil-González, J. Giraldo, A. Álvarez-Meza, A. Orozco-Gutiérrez, and M. A. Álvarez

Abstract*—The labeling process within a supervised learning task is usually carried out by an expert, which provides the ground truth (gold standard) for each sample. However, in many real-world applications, we typically have access to annotations provided by crowds holding different and unknown expertise levels. Learning from crowds intends to configure machine learning paradigms in the presence of multi-labelers, residing on two key assumptions: the labeler's performance does not depend on the input space, and independence among the annotators is imposed. Here, we propose the correlated chained Gaussian processes from multiple annotators–(CCGPMA) approach, which models each annotator's performance as a function of the input space and exploits the correlations among experts. Experimental results associated with classification and regression tasks show that our CCGPMA performs better modeling of the labelers' behaviour, indicating that it consistently outperforms other state-of-the-art learning from crowds approaches.

***Index Terms*—Multiple annotators, Correlated Chained Gaussian Processes, Variational inference, Semi-parametric latent factor model.**

I. INTRODUCTION

SUPERVISED learning requires that a domain expert labels the instances to built the gold standard (ground truth) (1). Yet, experts are scarce, or their time is expensive, not mentioning that the labeling task is tedious and time-consuming (2). As an alternative, the labeling is distributed through multiple heterogeneous annotators, who annotate part of the whole dataset by providing their version of the hidden ground truth (3). Recently, crowdsourcing platforms, i.e., Amazon Mechanical Turk– (AMT)[1], have been introduced to capture labels from multiple sources on large datasets efficiently. The attractiveness of these platforms lies in that, at a low cost, it is possible to obtain suitable quality labels. Indeed, in some cases, such a labeling process can compete with those provided by experts (4). However, in such multi-labeler scenario, each instance is matched with multiple annotations provided by different sources with unknown and diverse expertise, being difficult to apply traditional supervised learning algorithms (5). In this sense, *learning from crowds* has been introduced as a general framework from two main perspectives: to fit the labels from multiple annotators or to adapt the supervised learning algorithms (6).

J. Gil-González and A. Orozco are with the Universidad Tecnológica de Pereira, Colombia, 660003, e-mail:{jugil,aaog}@utp.edu.co

J. Giraldo and M. A.Álvarez are with the University of Sheffield, UK. email:{jjgiraldogutierrez1,mauricio.alvarez}@sheffield.ac.uk

A. Álvarez is with the Universidad Nacional de Colombia sede Manizales, 170001, Colombia. email: amalvarezme@unal.edu.co

[1]https://www.mturk.com/

The first approach is known in the literature as "label aggregation" or "truth inference", comprising the computation of a single hard label per sample as an estimation of the ground truth. The hard labels are then used to feed a standard supervised learning algorithm (7). The straightforward method is the so-called majority voting–(MV), and it has been used in different multi-labeler problems due to its simplicity (8). Still, MV assumes homogeneity in annotators' reliability, which is hardly feasible in real applications, e.g., experts vs. spammers. Furthermore, the consensus is profoundly impacted by incorrect labels and outliers (3). Conversely, more elaborated models have been considered to improve the estimation of the correct tag through the well-known Expectation-Maximization–(EM) framework and by facing the imbalanced labeling issue (9; 8).

The second approach jointly trains the supervised learning algorithm and models the annotators' behavior. It has been shown that such strategies lead to better performance compared to the ones belonging to label aggregation. Thus, the features used to train the learning algorithm provide valuable information to puzzle out the ground truth (10). The most representative work in this area is exposed in (11), which offers an EM-based framework to learn the parameters of a logistic regression classifier and model the annotators' behavior by computing their sensitivities and specificities. In fact, such a technique has inspired several models in the context of multi-labeler scenarios, including binary classification (12; 10), multi-class discrimination (7; 13), regression (14; 15), and sequence labeling (16). Furthermore, some works have addressed the multi-labeler problem using deep learning approaches typically including an extra layer that codes the annotators' information (17; 18; 19).

Two main issues are still unsolved in the context of learning from crowds (20): we need to code the relationships between the input features and the labelers' performance while revealing relevant annotators' interdependencies. In general, the annotators' behavior is parametrized through a homogeneous constraint across the input samples. The latter assumption is not correct since an expert makes decisions based not only on his/her expertise but also on the features observed from raw data (11). Besides, it is widespread to consider independence in the annotators' labels, aiming to reduce the complexity of the model (21), or based on the fact that it is plausible to guarantee that each labeler performs the annotation process individually (22). However, this assumption is not true since there may exist correlations among the annotators (23). For example, if the sources are humans, the independence assumption is hardly feasible because knowledge is a social construction; then, people's decisions will be correlated because they share information or belong to a particular school of

thought (24; 25). Now, if we consider that the sources are algorithms, where some of them gather the same math principle, there likely exists a correlation in their labels (26).

In this work, we propose a probabilistic model, named the correlated chained Gaussian Processes for multiple annotators (CCGPMA), to jointly build a prediction algorithm applicable to classification and regression tasks. CCGPMA is based on the chained GPs model–(CGP) (27), which is a Multi-GPs framework where the parameters of an arbitrary likelihood function are modeled with multiple independent GPs (one GP prior per parameter). Unlike CGP, we consider that multiple correlated GPs model the likelihood's parameters. For doing so, we take as a basis the ideas from a Multi-output GP–(MOGP) regression (28), where each output is coded as a weighted sum of shared latent functions via a semi-parametric latent factor model–(SLFM) (29). In contrast to the MOGP, we do not have multiple outputs but multiple functions chained to the given likelihood parameters. From the multiple annotators' point of view, the likelihood parameters are related to the labelers' behavior; thereby, CCGPMA models the labelers' behavior as a function of the input features while also taking into account annotators' interdependencies. Moreover, our proposal is based on the so-called inducing variables framework (30) in combination with stochastic variational inference (31). To the best of our knowledge, this is the first attempt to build a probabilistic approach to model the labelers' behavior as a function of the input features while also considering annotators' interdependencies. Achieved results, using both simulated and real-world data, show how our method can deal with both regression and classification problems from multi-labelers data.

The remainder is organized as follows. Section 2 exposes the related work and the main contributions of the proposal. Section 3 describes the methods. Sections 4 and 5 present the experiments and discuss the results. Finally, Section 6 outlines the conclusions and future work.

II. RELATED WORK AND MAIN CONTRIBUTIONS

Most of the learning from crowds-based methods aim to model the annotators' behavior based on the accuracy (32), the confusion matrix (13), the error variance (11), and the bias (15). Concerning this, the expert parameters are modeled as fixed points (12), or as random variables, where it is considered that such parameters are homogeneous across the input data (7).

The first attempt to analyze the relationship between the annotators' parameters and the input features is the work in (23). The authors propose an approach for binary classification with multiple labelers, where the input data is represented by a defined cluster using a Gaussian Mixture Model–(GMM). The approach assumes that the annotators exhibit a particular performance measured in terms of sensitivity and specificity for each group. However, the model does not consider the information from multiple experts as an input for the GMM, yielding variations in the labelers' parameters. Similarly, in (33), the authors propose a binary classification algorithm that employs two probability models to code the annotators' performance as a function of the input space, namely a Bernoulli and a Gaussian distribution. The parameters of these

distributions are computed via Logistic regression. Nonetheless, a linear dependence between the labeler expertise and the input space is assumed, which may not be appropriate because of the data structure's nonlinearities. For example, if we consider online annotators assessing some documents, they may have different labeling accuracy. Such differences may rely on whether they are more familiar with some specific topics related to studied documents (34). Authors in (35) offer a GP-based regression with multiple annotators. An additional GP models the annotators' parameters as a nonlinear function of the input space. Yet, the inference is carried out based on maximum a posteriori (MAP), without including the uncertainty of the posterior distribution.

On the other hand, it has been shown that the relaxation of the annotators' independence restriction can improve the ground truth estimation (23; 20). To the best of our knowledge, only two works address such an issue. First, the authors in (26) describe an approach to deal with regression problems, where the labelers' behavior is modeled using a multivariate Gaussian distribution. Thus, the annotators' interdependencies are coded in the covariance matrix. Further, in (36), the authors propose a binary classification method based on a weighted combination of classifiers. In turn, the weights are estimated by using a kernel alignment-based algorithm considering dependencies among the labelers.

Here, we propose a GPs-based framework to face classification and regression settings with multiple annotators. Our proposal follows the line of the works in (12; 14; 10; 7; 37) in the sense that we are modeling the unknown ground truth trough a GP prior. However, while such approaches code the annotators' parameters as fixed points (12; 14); or as random variables (10; 7; 37); we model them as random processes to take into account dependencies between the input space and the labelers' behavior. Besides, our CCGPMA shares some similarities with the works in (33; 35), because we aim to model the dependencies between the input features and the labelers' performance. Our method is also similar to the works in (26; 36), because they assume dependencies in the annotators' labels. In contrast, CCGPMA is the only one that includes both assumptions to code the annotators' behavior. Of note, we highlight that our proposal codes inconsistent annotations, being robust against outliers. Namely, CCGPMA can estimate the annotators' performance for every region in the input space; meanwhile, state-of-the-art techniques assess it based on a conventional averaging (15; 7; 10). Table I summarizes the key insights of our CCGPMA and state-of-the-art approaches.

III. METHODS

A. *Chained* Gaussian processes

Let us consider an input-output dataset $\mathcal{D} = \{\boldsymbol{X} \in \mathcal{X}, \boldsymbol{y} \in \mathcal{Y}\}$, where $\boldsymbol{X} = \left\{\boldsymbol{x}_n \in \mathcal{X} \subseteq \mathbb{R}^P\right\}_{n=1}^N$ and $\boldsymbol{y} = \{y_n \in \mathcal{Y}\}_{n=1}^N$. In turn, let a GP be a collection of random variables $f(\boldsymbol{x})$ indexed by the input samples $\boldsymbol{x} \in \mathcal{X}$ holding a joint multivariate Gaussian distribution (39). A GP is defined by its mean $m(\boldsymbol{x}) = \mathbb{E}[f(\boldsymbol{x})]$ (we consider $m(\boldsymbol{x}) = 0$) and covariance function $\kappa_f(\boldsymbol{x}, \boldsymbol{x}') = \mathbb{E}[(f(\boldsymbol{x}) - m(\boldsymbol{x}))(f(\boldsymbol{x}') - m(\boldsymbol{x}'))]$, where $\kappa_f : \mathcal{X} \times \mathcal{X} \to \mathbb{R}$ is a given kernel function and $\boldsymbol{x}' \in \mathcal{X}$, yielding:

TABLE I
SURVEY OF RELEVANT SUPERVISED LEARNING MODELS DEVOTED TO MULTIPLE ANNOTATORS.

Source	Data type	Type of model	Modeling the annotator's expertise	Expertise as a function of the input space	Modeling the annotators' inter-dependencies
Raykar et al., 2010 (11)	Regression-Binary-Categorical	Probabilistic	✓	✗	✗
Zhang and Obradovic, 2011 (23)	Binary	Probabilistic	✓	✓	✗
Xiao et al., 2013 (35)	Regression	Probabilistic	✓	✓	✗
Yan et al., 2014 (33)	Binary	Probabilistic	✓	✓	✗
Wang and Bi, 2016 (34)	Binary	Deterministic	✓	✓	✗
Rodrigues et al., 2017 (15)	Regression-Binary-Categorical	Probabilistic	✓	✗	✗
Gil-Gonzalez et al., 2018 (36)	Binary	Deterministic	✓	✗	✓
Hua et al., 2018 (38)	Binary-Categorical	Deterministic	✓	✗	✗
Ruiz et al., 2019 (10)	Binary	Probabilistic	✓	✗	✗
Morales- Alvarez et al., 2019 (7)	Binary	Probabilistic	✓	✗	✗
Zhu et al., 2019 (26)	Regression	Probabilistic	✓	✗	✓
Proposal-(CCGPMA)	Regression-Binary-Categorical	Probabilistic	✓	✓	✓

$$f(\boldsymbol{x}) \sim \mathcal{GP}(0, \kappa_f(\boldsymbol{x}, \boldsymbol{x}')). \tag{1}$$

If we consider the finite set of inputs in $\boldsymbol{X}$, then $\boldsymbol{f} = [f(\boldsymbol{x}_1), \ldots, f(\boldsymbol{x}_N)]^\top \in \mathbb{R}^N$ is drawn for a multivariate Gaussian distribution $\boldsymbol{f} \sim \mathcal{N}(\boldsymbol{f}|\boldsymbol{0}, \boldsymbol{K}_{ff})$, where $\boldsymbol{K}_{ff} \in \mathbb{R}^{N \times N}$ is the covariance matrix formed by the evaluation of $\kappa_f(\cdot, \cdot)$ over the input set $\boldsymbol{X}$.

Accordingly, using GPs for modeling the input-output data collection $\mathcal{D}$ consists of constructing a joint distribution between a given likelihood function and one or multiple GP-based priors. To code each likelihood parameter as a random process, we employ the so-called chained GP–(CGP) that attaches such parameters to multiple independent GP priors, as follows (27):

$$p(\boldsymbol{y}, \hat{\boldsymbol{f}}|\boldsymbol{X}) = \prod_{n=1}^{N} p(y_n|\theta_1(\boldsymbol{x}_n), \ldots, \theta_J(\boldsymbol{x}_n)) \times \cdots$$
$$\cdots \times \prod_{j=1}^{J} \mathcal{N}(\boldsymbol{f}_j|\boldsymbol{0}, \boldsymbol{K}_{\boldsymbol{f}_j \boldsymbol{f}_j}), \tag{2}$$

where each $\{\theta_j(\boldsymbol{x}) \in \mathcal{M}_j\}_{j=1}^J$ represents the likelihood's parameters, being $J \in \mathbb{N}$ the number of parameters to represent the likelihood. Besides, each $\theta_j(\boldsymbol{x})$ holds a non-linear mapping from a GP prior, e.g., $\theta_j(\boldsymbol{x}) = h_j(f_j(\boldsymbol{x}))$, where $h_j : \mathbb{R} \to \mathcal{M}_j$ is a deterministic function that maps each latent function–(LF) $f_j(\boldsymbol{x})$, to the appropriate domain $\mathcal{M}_j$. Moreover, $\boldsymbol{f}_j = [f_j(\boldsymbol{x}_1), \ldots, f_j(\boldsymbol{x}_N)]^\top \in \mathbb{R}^N$ is a LF vector that follows a GP prior, and $\hat{\boldsymbol{f}} = [\boldsymbol{f}_1, \ldots, \boldsymbol{f}_J]^\top \in \mathbb{R}^{NJ}$. $\boldsymbol{K}_{\boldsymbol{f}_j \boldsymbol{f}_j} \in \mathbb{R}^{N \times N}$ is the covariance matrix belonging to the j-th GP prior, which is computed based on the kernel function $\kappa_j : \mathcal{X} \times \mathcal{X} \to \mathbb{R}$. The non-parametric formulation of a GP introduces computational loads through the inference process. For instance, considering that the dataset $\mathcal{D}$ configures a regression problem, a GP modeling involves a computational complexity of $\mathcal{O}(N^3)$ to invert the matrix $\boldsymbol{K}_{\boldsymbol{f}_j \boldsymbol{f}_j}$ (39). A common approach to reduce such computational complexity is to augment the GP prior with a set of $M << N$ inducing variables (40), $\boldsymbol{u}_j = [f_j(\boldsymbol{z}_1^j), \ldots, f_j(\boldsymbol{z}_M^j)]^\top \in \mathbb{R}^M$ through additional evaluations of $f_j(\cdot)$ at unknown locations $\boldsymbol{Z}_j = [\boldsymbol{z}_1^j, \ldots, \boldsymbol{z}_M^j] \in$

$\mathbb{R}^{M \times P}$, which decreases the GP's computational complexity to $\mathcal{O}(NM^2)$. Further, the following augmented GP prior arises:

$$p(\boldsymbol{f}_j, \boldsymbol{u}_j) = \mathcal{N}\left(\begin{bmatrix} \boldsymbol{f}_j \\ \boldsymbol{u}_j \end{bmatrix} \middle| \boldsymbol{0}, \begin{bmatrix} \boldsymbol{K}_{\boldsymbol{f}_j \boldsymbol{f}_j} & \boldsymbol{K}_{\boldsymbol{f}_j \boldsymbol{u}_j} \\ \boldsymbol{K}_{\boldsymbol{u}_j \boldsymbol{f}_j} & \boldsymbol{K}_{\boldsymbol{u}_j \boldsymbol{u}_j} \end{bmatrix}\right), \tag{3}$$

where $\boldsymbol{K}_{\boldsymbol{f}_j \boldsymbol{u}_j} \in \mathbb{R}^{N \times M}$ is the cross-covariance matrix formed by the evaluation of the kernel function $\kappa_j(\cdot, \cdot)$ between $\boldsymbol{X}$ and $\boldsymbol{Z}_j$. Likewise, $\boldsymbol{K}_{\boldsymbol{u}_j \boldsymbol{u}_j} \in \mathbb{R}^{M \times M}$ is the inducing points-based covariance matrix. Then, the distribution of $\boldsymbol{f}_j$ conditioned to the inducing points $\boldsymbol{u}_j$ can be written as:

$$p(\boldsymbol{f}_j|\boldsymbol{u}_j) = \mathcal{N}\left(\boldsymbol{f}_j|\boldsymbol{K}_{\boldsymbol{f}_j \boldsymbol{u}_j} \boldsymbol{K}_{\boldsymbol{u}_j \boldsymbol{u}_j}^{-1} \boldsymbol{u}_j, \boldsymbol{K}_{\boldsymbol{f}_j \boldsymbol{f}_j} - \cdots \right. \tag{4}$$
$$\left. \cdots - \boldsymbol{K}_{\boldsymbol{f}_j \boldsymbol{u}_j} \boldsymbol{K}_{\boldsymbol{u}_j \boldsymbol{u}_j}^{-1} \boldsymbol{K}_{\boldsymbol{u}_j \boldsymbol{f}_j}\right),$$
$$p(\boldsymbol{u}_j) = \mathcal{N}\left(\boldsymbol{u}_j|\boldsymbol{0}, \boldsymbol{K}_{\boldsymbol{u}_j \boldsymbol{u}_j}\right). \tag{5}$$

In most cases Eqs. (4) and (5) are non-conjugate to the likelihood, finding the posterior distribution $p(\boldsymbol{f}, \mathbf{u}|\mathbf{y})$ is not tractable analytically; therefore, we resort to a deterministic approximation of the posterior distribution using variational inference. Hence, the actual posterior can be approximated by a parametrized variational distribution $p(\hat{\boldsymbol{f}}, \boldsymbol{u}|\boldsymbol{y}) \approx q(\hat{\boldsymbol{f}}, \boldsymbol{u})$, as:

$$q(\boldsymbol{f}, \boldsymbol{u}) = p(\boldsymbol{f}|\boldsymbol{u})q(\boldsymbol{u}) = \prod_{j=1}^{J} p(\boldsymbol{f}_j|\boldsymbol{u}_j)q(\boldsymbol{u}_j), \tag{6}$$

where $\boldsymbol{u} = [\boldsymbol{u}_1^\top, \ldots, \boldsymbol{u}_J^\top]^\top \in \mathbb{R}^{MJ}$; moreover, $p(\boldsymbol{f}_j|\boldsymbol{u}_j)$ is defined in Eq. (4), and $q(\boldsymbol{u})$ is the posterior approximation over the inducing variables:

$$q(\boldsymbol{u}) = \prod_{j=1}^{J} q(\boldsymbol{u}_j) = \prod_{j=1}^{J} \mathcal{N}\left(\boldsymbol{u}_j|\boldsymbol{m}_j, \boldsymbol{V}_j\right). \tag{7}$$

The approximation for the posterior distribution comprises the estimation of the following variational parameters: the mean vectors $\boldsymbol{m}_j \in \mathbb{R}^M$ and the covariance matrices $\boldsymbol{V}_j \in \mathbb{R}^{M \times M}$. Such an assessment is carried out by maximizing an evidence lower bound–(ELBO). Thereby, assuming that the instances $\boldsymbol{x}_n$ are independently sampled, the ELBO can be derived as:

$$\mathcal{L} = \sum_{n=1}^{N} \mathbb{E}_{q(\boldsymbol{f}_1),\ldots,q(\boldsymbol{f}_J)} \left[\log p(y_n|\theta_{1,n},\ldots,\theta_{J,n}) - \cdots \right.$$
$$\cdots - \sum_{j=1}^{J} \mathbb{D}_{KL}(q(\boldsymbol{u}_j)||p(\boldsymbol{u}_j)), \quad (8)$$

where $\mathbb{D}_{KL}(\cdot||\cdot)$ is the Kullback-Leibler divergence and $q(\boldsymbol{f}_j)$ is defined as follows:

$$q(\boldsymbol{f}_j) = \int p(\boldsymbol{f}_j|\boldsymbol{u}_j)q(\boldsymbol{u}_j)d\boldsymbol{u}_j. \quad (9)$$

B. Correlated chained Gaussian processes

From Section III-A, we note that the CGP model assumes independence between priors, thereby lacking a correlation structure between GPs. As mentioned before, we consider that the annotators are correlated. We will enable this aspect of the model by assuming dependencies among the latent parameters of the chained GP. In particular, we introduce the correlated chained GPs–(CCGP) to model correlations between the GP latent functions, which are supposed to be generated from a semi-parametric latent factor model–(SLFM) (29):

$$f_j(\boldsymbol{x}_n) = \sum_{q=1}^{Q} w_{j,q}\mu_q(\boldsymbol{x}_n), \quad (10)$$

where $f_j : \mathcal{X} \to \mathbb{R}$ is an LF, $\mu_q(\cdot) \sim \mathcal{GP}(0, k_q(\cdot,\cdot))$ with $k_q : \mathcal{X} \times \mathcal{X} \to \mathbb{R}$ being a kernel function, and $w_{j,q} \in \mathbb{R}$ is a combination coefficient ($Q \in \mathbb{N}$). Here, each LF is chained to the likelihood's parameters to extend the joint distribution in Eq. (2) as follows:

$$p(\boldsymbol{y}, \hat{\boldsymbol{f}}, \boldsymbol{u}|\boldsymbol{X}) = p(\boldsymbol{y}|\boldsymbol{\theta}) \prod_{j=1}^{J} p(\boldsymbol{f}_j|\boldsymbol{u})p(\boldsymbol{u}), \quad (11)$$

where $\boldsymbol{\theta} = [\boldsymbol{\theta}_1,\ldots,\boldsymbol{\theta}_J]^\top \in \mathbb{R}^{NJ}$ holds the model's parameters and $\boldsymbol{\theta}_j = [\theta_j(\boldsymbol{x}_1),\ldots,\theta_j(\boldsymbol{x}_N)]^\top \in \mathbb{R}^N$ relates the j-th parameter with the input space. Our CCGP employs the inducing variables-based method for sparse approximations of GPs (40). For each $\mu_q(\cdot)$, we introduce a set of $M \leq N$ "pseudo variables" $\boldsymbol{u}_q = [\mu_q(\boldsymbol{z}_1^q),\ldots,\mu_q(\boldsymbol{z}_M^q)]^\top \in \mathbb{R}^M$ through evaluations of $\mu_q(\cdot)$ at unknown locations $\boldsymbol{Z}_q = [\boldsymbol{z}_1^q,\ldots,\boldsymbol{z}_M^q] \in \mathbb{R}^{M \times P}$. Note that $\boldsymbol{u} = \left[\boldsymbol{u}_1^\top,\ldots,\boldsymbol{u}_Q^\top\right]^\top \in \mathbb{R}^{QM}$, yielding:

$$p(\boldsymbol{f}_j|\boldsymbol{u}) = \mathcal{N}\left(\boldsymbol{f}_j|\boldsymbol{K}_{\boldsymbol{f}_j\boldsymbol{u}}\boldsymbol{K}_{\boldsymbol{u}\boldsymbol{u}}^{-1}\boldsymbol{u}, \boldsymbol{K}_{\boldsymbol{f}_j\boldsymbol{f}_j} - \cdots \right.$$
$$\cdots - \boldsymbol{K}_{\boldsymbol{f}_j\boldsymbol{u}}\boldsymbol{K}_{\boldsymbol{u}\boldsymbol{u}}^{-1}\boldsymbol{K}_{\boldsymbol{u}\boldsymbol{f}_j}\right), \quad (12)$$
$$p(\boldsymbol{u}) = \mathcal{N}\left(\boldsymbol{u}|\boldsymbol{0}, \boldsymbol{K}_{\boldsymbol{u}\boldsymbol{u}}\right) = \prod_{q=1}^{Q} \mathcal{N}(\boldsymbol{u}_q|\boldsymbol{0}, \boldsymbol{K}_{\boldsymbol{u}_q\boldsymbol{u}_q}), \quad (13)$$

where $\boldsymbol{K}_{\boldsymbol{u}\boldsymbol{u}} \in \mathbb{R}^{QM \times QM}$ is a block-diagonal matrix with blocks $\boldsymbol{K}_{\boldsymbol{u}_q\boldsymbol{u}_q} \in \mathbb{R}^{M \times M}$, based on the kernel function $\kappa_q(\cdot,\cdot)$. The covariance matrix $\boldsymbol{K}_{\boldsymbol{f}_j\boldsymbol{f}_j} \in \mathbb{R}^{N \times N}$ holds

elements $\sum_{q=1}^{Q} w_{j,q}w_{j,q}\kappa_q(\boldsymbol{x}_n,\boldsymbol{x}_{n'})$, with $\boldsymbol{x}_n, \boldsymbol{x}_{n'} \in \boldsymbol{X}$. Likewise, $\boldsymbol{K}_{\boldsymbol{f}_j\boldsymbol{u}} = [\boldsymbol{K}_{\boldsymbol{f}_j\boldsymbol{u}_1},\ldots,\boldsymbol{K}_{\boldsymbol{f}_j\boldsymbol{u}_Q}] \in \mathbb{R}^{N \times QM}$, where $\boldsymbol{K}_{\boldsymbol{f}_j\boldsymbol{u}_q} \in \mathbb{R}^{N \times M}$ gathers elements $w_{j,q}\kappa_q(\boldsymbol{x}_n,\boldsymbol{z}_m^q)$, $m \in \{1,\ldots,M\}$. Alike CGP, in most cases, the CCGP posterior distribution $p(\hat{\boldsymbol{f}}, \boldsymbol{u}|\boldsymbol{y})$ has not an analytical solution, so the actual posterior can be approximated by a parametrized variational distribution $p(\hat{\boldsymbol{f}}, \boldsymbol{u}|\boldsymbol{y}) \approx q(\hat{\boldsymbol{f}}, \boldsymbol{u})$, as:

$$q(\hat{\boldsymbol{f}}, \boldsymbol{u}) = p(\hat{\boldsymbol{f}}|\boldsymbol{u})q(\boldsymbol{u}) = \prod_{j=1}^{J} p(\boldsymbol{f}_j|\boldsymbol{u}) \prod_{q=1}^{Q} q(\boldsymbol{u}_q), \quad (14)$$

where $p(\boldsymbol{f}_j|\boldsymbol{u})$ is given by Eq. (12), $q(\boldsymbol{u}_q) = \mathcal{N}(\boldsymbol{u}_q|\boldsymbol{m}_q, \boldsymbol{V}_q)$, and $q(\boldsymbol{u}) = \mathcal{N}(\boldsymbol{u}|\boldsymbol{m}, \boldsymbol{V})$. Also, $\boldsymbol{m}_q \in \mathbb{R}^M$, and $\boldsymbol{V}_q \in \mathbb{R}^{M \times M}$ are respectively the mean and covariance of variational distribution $q(\boldsymbol{u}_q)$; similarly, $\boldsymbol{m} = [\boldsymbol{m}_1^\top,\ldots,\boldsymbol{m}_Q^\top]^\top \in \mathbb{R}^{QM}$, and $\boldsymbol{V} \in \mathbb{R}^{QM \times QM}$ is a block-diagonal matrix with blocks given by the covariance matrices $\boldsymbol{V}_q$. We remark that the variational approximation given by Eq. (14) is not uncommon, and it has been used in several GPs models, including (27; 41). The approximation for the posterior distribution comprises the computation of the following variational parameters: the mean vectors $\{\boldsymbol{m}_q\}_{q=1}^{Q}$ and the covariance matrices $\{\boldsymbol{V}_q\}_{q=1}^{Q}$. Such an estimation is carried out by maximizing an evidence lower bound–(ELBO), which is given as:

$$\mathcal{L} = \sum_{n=1}^{N} \mathbb{E}_{q(\boldsymbol{f}_1),\ldots,q(\boldsymbol{f}_J)} \left[\log p(y_n|\theta_{1,n},\ldots,\theta_{J,n}) - \cdots \right.$$
$$\cdots - \sum_{q=1}^{Q} \mathbb{D}_{KL}(q(\boldsymbol{u}_q)||p(\boldsymbol{u}_q)), \quad (15)$$

where $\theta_{j,n} = \theta_j(\boldsymbol{x}_n)$, with $j \in \{1,\ldots,J\}$, and $\mathbb{D}_{KL}(\cdot||\cdot)$ is the Kullback-Leibler divergence and $q(\boldsymbol{f}_j)$ is defined as follows:

$$q(\boldsymbol{f}_j) = \mathcal{N}(\boldsymbol{f}_j|\boldsymbol{K}_{\boldsymbol{f}_j\boldsymbol{u}}\boldsymbol{K}_{\boldsymbol{u}\boldsymbol{u}}^{-1}\boldsymbol{m}, \boldsymbol{K}_{\boldsymbol{f}_j\boldsymbol{f}_j} + \cdots$$
$$\cdots + \boldsymbol{K}_{\boldsymbol{f}_j\boldsymbol{u}}\boldsymbol{K}_{\boldsymbol{u}\boldsymbol{u}}^{-1}(\boldsymbol{V} - \boldsymbol{K}_{\boldsymbol{u}\boldsymbol{u}})\boldsymbol{K}_{\boldsymbol{u}\boldsymbol{u}}^{-1}\boldsymbol{K}_{\boldsymbol{u}\boldsymbol{f}_j}). \quad (16)$$

Yet, in presence of non-Gaussian likelihoods, the computation of the variational expectations–(VEs) in Eq. (15) cannot be solved analytically (27; 41). Hence, aiming to model different data types, i.e., classification and regression tasks, we need to find a generic alternative to solve the integrals related to these expectations. In that sense, we use the Gaussian-Hermite quadratures approach as in (40; 27). We remark such ELBO is used to infer the model's hyperparameters such as the inducing points, the kernel hyperparameters, and the combination factors $w_{j,q}$ Eq. (10). It is worth mentioning that the CCGPs objective functions exhibit an ELBO that allows Stochastic Variational Inference–(SVI) (42). Hence, the optimization is solved through a *mini-batch*-based approach from noisy estimates of the global objective gradient, which allows dealing with large scale datasets (40; 27; 41). Finally, we notice that the computational complexity for our CCGP is similar to the model in (41). Accordingly, it is dominated by the inversion of $\boldsymbol{K}_{\boldsymbol{u}\boldsymbol{u}}$ with $\mathcal{O}(QM^3)$ and products like $\boldsymbol{K}_{\hat{\boldsymbol{f}}\boldsymbol{u}}$ with $\mathcal{O}(JNQM^2)$.

C. Correlated chained GP for multiple annotators-CCGPMA

Let us consider that a predefined panel of $R \in \mathbb{N}$ annotators (with different and unknown levels of expertise) label a given dataset of N instances. It is common to find that the each annotator r only labels $|N_r| \leq N$ samples, being $|N_r|$ the cardinality of the set $N_r \subseteq \{1, \ldots, N\}$ that contains the indexes of samples labeled by the r-th annotator. Besides, we define the set $R_n \subseteq \{1, \ldots, R\}$ holding the indexes of annotators that labeled the n-th instance. The input-output set is coupled within a multiple annotators scenario as $\mathcal{D} = \{\boldsymbol{X}, \boldsymbol{Y} = \{y_n^r\}_{n \in N, r \in R_n}\}$, where $y_n^r \in \mathcal{Y}$ is the output given by labeler r to the sample n; accordingly, our main aims are: *i)* to code each labeler's performance as a function of the input space and taking into account inter-annotator dependencies, and *ii)* to predict the true output $y_* \in \mathcal{Y}$ of a new instance $\boldsymbol{x}_* \in \mathbb{R}^P$. We highlight that to achieve such objectives no extra information about the annotators' behaviour is provided (e.g., extra labels or information about her/his experience).

1) Classification: To model categorical data from multiple annotators with K classes ($\mathcal{Y} = \{1, \ldots, K\}$) using our CCGPMA, we use the framework proposed in (32), which introduces a binary variable $\lambda_n^r \in \{0, 1\}$ representing the r-th labeler's reliability as a function of each sample $\boldsymbol{x}_n$. If $\lambda_n^r = 1$, the r-th annotator is supposed to provide the actual label, yielding to a categorical distribution. Conversely, $\lambda_n^r = 0$ indicates that the r-th annotator gives an incorrect output, which is modeled by a uniform distribution. Therefore, the likelihood function is given as:

$$p(\boldsymbol{Y}|\boldsymbol{\theta}) = \prod_{n=1}^{N} \prod_{r \in R_n} \left(\prod_{k=1}^{K} \zeta_{k,n}^{\delta(y_n^r, k)} \right)^{\lambda_n^r} \left(\frac{1}{K} \right)^{(1-\lambda_n^r)}, \quad (17)$$

where $\delta(y_n^r, k) = 1$, if $y_n^r = k$, otherwise $\delta(y_n^r, k) = 0$. Besides, $\zeta_{k,n} = p(y_n^r = k | \lambda_n^r = 1)$ is an estimation of the unknown ground truth. Accordingly, $J = K + R$ LFs are required within our CCGPMA approach, aiming to model the likelihood parameters $\boldsymbol{\theta}$. In particular, K LFs are used to model $\zeta_{k,n}$ based on a softmax function ι as:

$$\zeta_{k,n} = \iota(f_k(\boldsymbol{x}_n)) = \frac{\exp(f_k(\boldsymbol{x}_n))}{\sum_{j=1}^{K} \exp(f_j(\boldsymbol{x}_n))}. \quad (18)$$

Besides, R LFs are utilized to compute each λ_n^r from a step function; therefore, $\lambda_n^r = 1$ if $f_{l_r}(\boldsymbol{x}_n) \geq 0$, otherwise, $\lambda_n^r = 0$ ($r \in \{1, \ldots R\}$). $l_r = K + r \in \{K+1, \ldots J\}$ indexes the r-th annotator' LF. Of note, we approximate the step function through the well-known sigmoid function ς to avoid discontinuities and favor the CCGPMA implementation. Alike to CCGP, we use variational inference to approximate the posterior distribution of our CCGPMA. In consequence, the actual posterior $p(\hat{\boldsymbol{f}}, \boldsymbol{u}|\boldsymbol{Y})$ is approximated following Eq. (14). Besides, we can derive a CCGPMA ELBO, yielding:

$$\mathcal{L} = \sum_{n=1}^{N} \sum_{r \in R_n} \mathbb{E}_{q(\boldsymbol{f}_1), \ldots, q(\boldsymbol{f}_J)} \left[\log p(y_n^r | \theta_{1,n}, \ldots, \theta_{J,n}) \right] - \cdots$$
$$\cdots - \sum_{q=1}^{Q} \mathbb{D}_{KL}(q(\boldsymbol{u}_q)||p(\boldsymbol{u}_q)), \quad (19)$$

where for the classification case, we have

$$p(y_n^r | \theta_{1,n}, \ldots, \theta_{J,n}) = \left(\prod_{k=1}^{K} \zeta_{k,n}^{\delta(y_n^r, k)} \right)^{\lambda_n^r} \left(\frac{1}{K} \right)^{(1-\lambda_n^r)}. \quad (20)$$

Finally, given a new sample $\boldsymbol{x}_*$, we are interested in the mean and variance for predictive distributions related to the ground truth $\zeta_{k,*} = p(y_* = k | \boldsymbol{x}_*, \hat{\boldsymbol{f}}, \boldsymbol{u})$, and the labelers' reliabilities λ_*^r. Accordingly, for $\zeta_{k,*}$ we obtain

$$\mathbb{E}[\zeta_{k*}] \approx \int \iota(f_k(\boldsymbol{x}_*)) q(\boldsymbol{f}_*) d\boldsymbol{f}_*, \quad (21)$$

where $q(\boldsymbol{f}_*) = \int p(\boldsymbol{f}_*|\boldsymbol{u}) q(\boldsymbol{u}) d\boldsymbol{u}$. Similarly, for the predictive variance of $\zeta_{k,*}$, we use the expression $\text{Var}[\zeta_{k,*}] = \mathbb{E}[\zeta_{k,*}^2] - \mathbb{E}[\zeta_{k,*}]^2$; hence, we need to compute $\mathbb{E}[\zeta_{k,*}^2]$ as

$$\mathbb{E}[\zeta_{k*}^2] \approx \int \iota(f_k(\boldsymbol{x}_*))^2 q(\boldsymbol{f}_*) d\boldsymbol{f}_*. \quad (22)$$

On the other hand, regarding the predictive mean and variance for λ_*^r, we have

$$\mathbb{E}[\lambda_*^r] = \int \varsigma(f_{l_r,*}) q(\boldsymbol{f}_*) d\boldsymbol{f}_*. \quad (23)$$

For the variance of λ_*^r, we use the expression $\text{Var}[\lambda_*^r] = \mathbb{E}[(\lambda_*^r)^2] - \mathbb{E}[\lambda_*^r]^2$; hence, we need to compute

$$\mathbb{E}[(\lambda_*^r)^2] = \int \varsigma(f_{l_r,*})^2 q(\boldsymbol{f}_*) d\boldsymbol{f}_*. \quad (24)$$

In this case, integrals in Eqs. (21) to (24) have not closed solution; hence, we approximate them using the Gaussian-Hermite quadrature.

2) Regression: For real-valued outputs, e.g., $\mathcal{Y} \subset \mathbb{R}$, we follow the multi-annotator model used in (11; 14; 35; 15), where each output y_n^r is considered to be a corrupted version of the hidden ground truth y_n. Then:

$$p(\boldsymbol{Y}|\boldsymbol{\theta}) = \prod_{n=1}^{N} \prod_{r \in R_n} \mathcal{N}\left(y_n^r | y_n, v_n^r\right), \quad (25)$$

where $v_n^r \in \mathbb{R}^+$ is the r-th annotator error-variance for the instance n. In turn, to model this likelihood function with CCGPMA, it is necessary to chain each likelihood's parameter to a latent function f_j. Thus, we require $J = R + 1$ LFs; one to model the hidden ground truth, such that $y_n = f_1(\boldsymbol{x}_n)$, and R LFs to model each error-variance $v_n^r = \exp(f_{l_r}(\boldsymbol{x}_n))$, with $r \in \{1, \ldots R\}$, and $l_r = r + 1 \in \{2, \ldots J\}$. Note that we use an exponential function to map from f_{l_r} to v_n^r, aiming

to guarantee $v_n^r > 0$ ($f_{l_r} \in \mathbb{R}$). Similar to the classification problem, the ELBO in regression settings is given by Eq. (19), where $p(y_n^r | \theta_{1,n}, \dots, \theta_{J,n}) = \mathcal{N}(y_n^r | y_n, v_n^r)$.

Now, given a new sample $\boldsymbol{x}_*$, we are interested in the mean and variances for predictive distributions concerning the ground truth y_*, and the labelers' error-variances v_*^r. First, for y_* we have that since $\mathbf{y} = \boldsymbol{f}_1$, the posterior distribution for y_* corresponds to $q(f_{1*})$, yielding:

$$\mathbb{E}[y_*] = \mu_{1,*} \tag{26}$$

$$\mathrm{Var}[y_*] = s_{1,*}, \tag{27}$$

where $\mu_{1,*}$, and $s_{1,*}$ are respectively the mean and variance of $q(f_{1*})$. Then, for v_*^r, we note that due to $\mathbf{v}_r = \exp(\boldsymbol{f}_{l_r})$, the posterior distribution for v_*^r follows a log-normal distribution with parameters $\mu_{l_r,*}$ and $s_{l_r,*}$, which respectively correspond to the mean and variance of $q(f_{l_r,*})$. In this sense, the mean and variance of v_*^r are given as:

$$\mathbb{E}[v_*^r] = \exp\left(\mu_{l_r,*} + \frac{s_{l_r,*}}{2}\right). \tag{28}$$

$$\mathrm{Var}[v_*^r] = \exp\left(2\mu_{l_r,*} + s_{l_r,*}\right)\left(\exp(s_{l_r,*}) - 1\right). \tag{29}$$

IV. EXPERIMENTAL SET-UP

In this section, we describe the experiments' configurations to validate our CCGPMA concerning multiple annotators classification and regression tasks.

A. Classification

1) Datasets and simulated/provided annotations: We test our approach using three types of datasets: *fully synthetic data*, *semi-synthetic data*, and *fully real datasets*.

First, we generate *fully synthetic data* as one-dimensional ($P = 1$) multi-class classification problem ($K = 3$). The input feature matrix $\boldsymbol{X}$ is built by randomly sampling $N = 100$ points from an uniform distribution within the interval $[0, 1]$. The true label for the n-th sample is generated by taking the $\arg\max_i\{t_{n,i} \,:\, i \in \{1, 2, 3\}\}$, where $t_{n,1} = \sin(2\pi x_n)$, $t_{n,2} = -\sin(2\pi x_n)$, and $t_{n,3} = -\sin(2\pi(x_n + 0.25)) + 0.5$. Besides, the test instances are obtained by extracting 200 equally spaced samples from the interval $[0, 1]$.

Second, to control the label generation, we build *semi-synthetic data* from seven datasets of the UCI repository[^2] focused on binary and multi class-classification: Wisconsin Breast Cancer Database–(breast), BUPA liver disorders (bupa), Johns Hopkins University Ionosphere database (ionosphere), Pima Indians Diabetes Database–(pima), Tic-Tac-Toe Endgame database–(tic-tac-toe), Occupancy Detection Data Set–(Occupancy), Skin Segmentation Data Set–(Skin), Wine Data set–(Wine), and Image Segmentation Data Set (Segmentation). Also, we test the publicly available bearing data collected by the Case Western Reserve University–(Western). The aim is to build a system to diagnose an electric motor's

[^2]: http://archive.ics.uci.edu/ml

TABLE II
TESTED DATASETS.

	Name	Number of features	Number of instances	Number of classes
fully synthetic	synthetic	1	100	3
semi-synthetic	Breast	9	683	2
	Bupa	6	345	2
	Ionosphere	34	351	2
	Pima	8	768	2
	Tic-tac-toe	9	958	2
	Occupancy	7	20560	2
	Skin	4	245057	2
	Western	7	3413	4
	Wine	13	178	3
	Segmentation	18	2310	7
fully real	Voice	13	218	2
	Music	124	1000	10

status based on two accelerometers. The feature extraction was performed as in (43).

Third, we evaluate our proposal on two *fully real datasets*, where both the input features and the annotations are captured from real-world problems. Namely, we use a bio-signal database, where the goal is to build a system to evaluate the presence/absence of voice pathologies. In particular, a subset ($N = 218$) of the Massachusetts Eye and Ear Infirmary Disordered Voice Database from the Kay Elemetrics company is utilized, which comprises voice records from healthy and different voice issues. Each signal is parametrized by the Mel-frequency cepstral coefficients (MFCC) to obtain an input space with $P = 13$. A set of physicians assess the voice quality by following the GRBAS protocol that comprises the evaluation of five qualitative scales: Grade of dysphonia–(G), Roughness–(R), Breathiness–(B), Asthenia–(A), and Strain–(S). For each perceptual scale, the specialist assigns a tag ranging from 0 (healthy voice) to 3 (severe disease) (44). Accordingly, we face five multi-class classification problems (one per scale). We follow the procedure in (36) to rewrite five binary classification tasks preserving the available ground truth (13). Further, we use the music genre data[^3], holding a collection of songs records labeled from one to ten depending on their music genre: classical, country, disco, hip-hop, jazz, rock, blues, reggae, pop, and metal. From this set, 700 samples were published randomly in the AMT platform to obtain labels from multiples sources (2946 annotations from 44 workers). Yet, we only consider the annotators who labeled at least 20% of the instances; thus, we use the information from $R = 7$ labelers. The feature extraction is performed by following the work by authors in (32), to obtain an input space with $P = 124$. Table II summarizes the tested datasets for the classification case.

Note that the *fully synthetic* and the *semi-synthetic* datasets do not hold real annotations. Therefore, it is necessary to simulate those labels as corrupted versions of the hidden ground truth. Here, the simulations are performed by assuming: i) dependencies among annotators, and ii) the labelers' performance is modeled as a function of the input features. In turn, an SLFM-based approach (termed SLFM-C) is used to build the labels, as follows:

– Define Q deterministic functions $\hat{\mu}_q : \mathcal{X} \to \mathbb{R}$, and their combination parameters $\hat{w}_{l_r,q} \in \mathbb{R}$, $\forall r \in R, n \in N$.

[^3]: http://fprodrigues.com/publications/learning-from-multiple-annotators-distinguishing-good-from-random-labelers/

TABLE III
A BRIEF OVERVIEW OF THE STATE-OF-THE-ART METHODS TESTED.

Algorithm	Description
GPC-GOLD	A GPC using the real labels (upper bound).
GPC-MV	A GPC using the MV of the labels as the ground truth.
MA-LFC-C (11)	A LRC with constant parameters across the input space.
MA-DGRL (32)	A multi-labeler approach that considers as latent variables the annotator performance.
MA-GPC (12)	A multi-labeler GPC, which is as an extension of MA-LFC.
MA-GPCV (7)	An extension of MA-GPC that includes variational inference and priors over the labelers' parameters.
MA-DL (18)	A Crowd Layer for DL, where the annotators' parameters are constant across the input space.
KAAR (36)	A kernel-based approach that employs a convex combination of classifiers and codes labelers dependencies.
CGPMA-C	A particular case of our CCGPMA for classification, where $Q = J$, and we fix $w_{j,q} = 1$, if $j = q$, otherwise $w_{j,q} = 0$.

– Compute $\hat{f}_{l_r,n} = \sum_{q=1}^{Q} \hat{w}_{l_r,q} \hat{\mu}_q(\hat{x}_n)$, where $\hat{x}_n \in \mathbb{R}$ is the n-th component of $\hat{x} \in \mathbb{R}^N$, being $\hat{x}$ the $1-$D representation of the input features in X by using the well-known t-distributed Stochastic Neighbor Embedding approach (45).

– Calculate $\hat{\lambda}_n^r = \varsigma(\hat{f}_{l_r,n})$, where $\varsigma(\cdot) \in [0, 1]$ is the sigmoid function.

– Finally, find the r-th label as $y_n^r = \begin{cases} y_n, & \text{if } \lambda_n^r \geq 0.5 \\ \tilde{y}_n, & \text{if } \lambda_n^r < 0.5 \end{cases}$, where $\tilde{y}_n$ is a flipped version of the actual label y_n.

2) Method comparison and performance metrics: The classification performance is assessed as the Area Under the Curve–(AUC). Further, the AUC is extended for multi-class settings, as discussed by authors in (46). We use a cross-validation scheme with 15 repetitions where 70% of the samples are utilized for training and the remaining 30% for testing (except for the music dataset training and testing sets are clearly defined). Table III displays the employed methods of the state-of-the-art for comparison purposes. The abreviations are fixed as: Gaussian Processes classifier (GPC), logistic regression classifier (LRC), majority voting (MV), multiple annotators (MA), Modelling annotators expertise (MAE), Learning from crowds (LFC), Distinguishing good from random labelers (DGRL), kernel alignment-based annotator relevance analysis (KAAR).

B. Regression

1) Datasets and simulated/provided annotations: We test our approach using three types of datasets: fully synthetic data, semi-synthetic data, and fully real datasets. First, We generate *fully synthetic data* as an one-dimensional regression problem where the ground truth for the n-th sample corresponds to $y_n = \sin(2\pi x_n)\sin(6\pi x_n)$, where the input matrix X is formed by randomly sampling 100 points within the range $[0, 1]$ from an uniform distribution. The test instances are obtained by extracting equally spaced samples from the interval $[0, 1]$. Second, to control the label generation (10), we build *semi-synthetic data* from six datasets related to regression tasks from the well-known UCI repository. We selected the following datasets: Auto MPG Data Set–(Auto), Bike Sharing Dataset Data Set–(Bike), Concrete Compressive Strength Data Set–(Concrete), The Boston Housing Dataset–(Housing),[4] Yacht

[4]See https://www.cs.toronto.edu/~delve/data/boston/bostonDetail.html for housing

TABLE IV
DATASETS FOR REGRESSION.

	Name	Number of features	Number of instances
fully synthetic	synthetic	1	100
semi-synthetic	Auto	8	398
	Bike	13	17389
	Concrete	9	1030
	Housing	13	506
	Yacht	6	308
	CT	384	53500
fully real	Music	124	1000

TABLE V
A BRIEF OVERVIEW OF STATE-OF-THE-ART METHODS TESTED FOR REGRESSION TASKS. GPR: GAUSSIAN PROCESSES REGRESSION, LR: LOGISTIC REGRESSION, AV: AVERAGE, MA: MULTIPLE ANNOTATORS, DL: DEEP LEARNING, LFCR: LEARNING FROM CROWDS FOR REGRESSION.

Algorithm	Description
GPR-GOLD	A GPR using the real labels (upper bound).
GPR-Av	A GPR using the average of the labels as the ground truth.
MA-LFCR (11)	A LR model for MA where the labelers' parameters are supposed to be constant across the input space.
MA-GPR (12)	A multi-labeler GPR, which is as an extension of MA-LFCR.
MA-DL (18)	A Crowd Layer for DL, where the annotators' parameters are constant across the input space.
CGPMA-R	A particular case of our CCGPMA for regression, where $Q = J$, and $w_{j,q} = 1$ if $j = q$, otherwise $w_{j,q} = 0$.

Hydrodynamics Data Set–(Yacht), and Relative location of CT slices on axial axis Data Set–(CT). Third, we evaluate our proposal on one *fully real dataset*. In particular, we use the Music dataset introduced in Section IV-A1. Notice that the music dataset configures a 10-class classification problem; however, in this experiment, we are using our CCGPMA with a likelihood function designed for real-valued labels Eq. (25). Such practice is not uncommon in machine learning, and it is usually known as "Least-square classification" (39). Table IV summarizes the tested datasets for the regression case.

As we pointed out previously, *fully synthetic* and *semi-synthetic* datasets do not hold real annotations. Thus, it is necessary to generate these labels synthetically as a version of the gold standard corrupted by Gaussian noise, i.e., $y_n^r = y_n + \epsilon_n^r$, where $\epsilon_n^r \sim \mathcal{N}(0, v_n^r)$, being v_n^r the r-th annotator error-variance for the sample n. Note that we are interested in modeling such an error-variance for the r-th annotator as a function of the input features, which is correlated with the other labelers' variances. In turn, an SLFM-based approach (termed SLFM-R) is used to build the labels, as follows:

- Define Q functions $\hat{\mu}_q : \mathcal{X} \to \mathbb{R}$, and the combination parameters $\hat{w}_{l_r,q} \in \mathbb{R}, \forall r, q$.
- Compute $\hat{f}_{l_r,n} = \sum_{q=1}^{Q} \hat{w}_{l_r,q} \hat{\mu}_q(\hat{x}_n)$, where $\hat{x}_n$ is the n-th component of $\hat{x} \in \mathbb{R}$, which is an $1-$D representation of input features X by using the t-distributed Stochastic Neighbor Embedding approach (45).
- Finally, determine $\hat{v}_n^r = \exp(\hat{f}_{l_r,n})$.

2) Method comparison and performance metrics: The quality assessment is carried out by estimating the regression performance as the coefficient of determination–(R^2). A cross-validation scheme is employed with 15 repetitions where 70% of the samples are utilized for training and the remaining

30% for testing (except for *fully synthetic dataset*, since it clearly defines the training and testing sets). Table V displays the employed methods of the state-of-the-art for comparison purposes. From Table V, we highlight that for the model MA-DL, the authors provided three different annotators' codification: MA-DL-B, where the bias for the annotators is measured; MA-DL-S, where the labelers' scale is computed; and measured; MA-DL-B+S, which is a version with both (18).

C. CCGPMA training

Overall, the Radial basis function–(RBF) kernel is preferred in both classification and regression tasks because of its universal approximating ability and mathematical tractability. Hence, for all GP-based approaches, the kernel functions are fixed as:

$$\kappa(\boldsymbol{x}_n, \boldsymbol{x}_{n'}) = \phi_1 \exp\left(\frac{-\|\boldsymbol{x}_n - \boldsymbol{x}_{n'}\|_2^2}{2\phi_2^2}\right), \quad (30)$$

where $\|\cdot\|^2$ stands for the L2 norm, $n, n' \in \{1, 2, \ldots, N\}$, and $\phi_1, \phi_2 \in \mathbb{R}^+$ are the kernel hyper-parameters. For concrete testing, we fix $\phi_1 = 1$, while ϕ_2 is estimated by optimizing the corresponding ELBO (as exposed in Eq. (19)). Moreover, for CGPMA, since each LF $f_j(\cdot)$ is linked to $u_q(\cdot)$, we fix $Q = R + K$, and $Q = R+1$ for classification and regression respectively. On the other hand, for CCGPMA, each $f_j(\cdot)$ is built as a convex combination of $\mu_q(\cdot)$ (see Eq. (10)); therefore, there is no restriction concerning Q. However, to make a fair comparison with CGPMA, we also fix $Q = R + K$ (classification), and $Q = R + 1$ (regression) in CCGPMA. For the *fully synthetic datasets*, we use $M = 10$ inducing points per latent function, and for the remaining experiments, we test with $M = 40$, and $M = 80$. For all the experiments, we use the ADADELTA included in the climin library with a mini-batch size of 100 samples to perform SVI. However, for small datasets ($N < 500$), we employ mini-batches with a size equal to the number of samples in the training set. Finally, for all experiments related to our CCGPMA, the variational parameters' initialization is carried out as follows: the variational mean is set $\boldsymbol{m}_q = \boldsymbol{0}, \forall q \in \{1, \ldots, Q\}$, where $\boldsymbol{0} \in \mathbb{R}^M$ is an all-zeros vector; the variational covariances $\boldsymbol{V}_q = \boldsymbol{I}, \forall q \in \{1, \ldots, Q\}$ are fixed as the identity matrix $\boldsymbol{I} \in \mathbb{R}^{M \times M}$. The CCGPMA's Python code is publicly available.[5]

V. RESULTS AND DISCUSSION

A. Classification

1) Fully synthetic data results.: We first perform a controlled experiment to test the CCGPMA capability when dealing with binary and multi-class classification. We use the *fully synthetic* dataset described in Section IV-A1. Besides, five labelers ($R = 5$) are simulated with different levels of expertise. To simulate the error-variances, we define $Q = 3$ $\hat{\mu}_q(\cdot)$ functions, yielding:

---

[5]https://github.com/juliangilg/CCGPMA

$$\hat{\mu}_1(x) = 4.5\cos(2\pi x + 1.5\pi) - 3\sin(4.3\pi x + 0.3\pi), \quad (31)$$
$$\hat{\mu}_2(x) = 4.5\cos(1.5\pi x + 0.5\pi) + 5\sin(3\pi x + 1.5\pi), \quad (32)$$
$$\hat{\mu}_3(x) = 1, \quad (33)$$

where $x \in [0, 1]$. Besides, the combination weights are gathered within the following combination matrix $\hat{\boldsymbol{W}} \in \mathbb{R}^{Q \times R}$:

$$\hat{\boldsymbol{W}} = \begin{bmatrix} 0.4 & 0.7 & -0.5 & 0.0 & -0.7 \\ 0.4 & -1.0 & -0.1 & -0.8 & 1.0 \\ 3.1 & -1.8 & -0.6 & -1.2 & 1.0 \end{bmatrix}, \quad (34)$$

holding elements $\hat{w}_{l_r,q}$. For visual inspection purposes, Fig. 1 shows the predictive label's probability–(PLP), $p(y_* = k|\boldsymbol{x}_*)$, and the AUC for all studied approaches regarding the *fully synthetic* data. Notice that for methods MA-GPC, MA-GPCV, and KAAR, we use the *one-vs-all* scheme to face this experiment (such methods were defined only for binary classification settings). Accordingly, for those models, the PLP corresponds to scores rather than probabilities. Besides, regarding the PLP of our CGPMA and CCGPMA, we provide the mean and variance for the predictive distribution $\zeta_{k,*} = p(y_* = k|\boldsymbol{x}_*, \hat{\boldsymbol{f}}, \boldsymbol{u})$, which are computed based on Eqs. (21) and (22). As seen in Fig. 1, KAAR, MA-GPC, and MA-GPCV presents a different shape than the ground truth; moreover, KAAR and MA-GPCV exhibit the worst AUC, even worse than the intuitive lower bound GPC-MV. We explain such conduct in the sense that these approaches are designed to deal with binary labels (36; 12; 10). To face such a problem, we use the *one-vs-all* scheme; still, it can lead to ambiguously classified regions (47). We note an akin predictive AUC concerning MA-DL methods and the linear approaches MA-LFC-C and MA-DGRL. Nonetheless, the linear techniques exhibit a PLP less similar to the Ground truth, which is due to MA-LFC-C and MA-DGRL only can deal with linearly separable data. Further, we analyze the results of our CGPMA-C and its particular enhancement CCGPMA-C. We remark that our methods' predictive AUC is pretty close to deep learning and linear models. Unlike them, our CGPMA-C and CCGPMA-C show the most accurate PLP compared with the absolute gold standard. CCGPMA-C behaves quite similarly to GPC-GOLD, which is the theoretical upper bound. Finally, from the GPC-MV, we do not identify notable differences with the rest of the approaches (excluding KAAR and MA-GPCV).

From the above, we recognize that analyzing both the predictive AUC and the PLP, our CCGPMA-C exhibits the best performance obtaining similar results compared with the intuitive upper bound (GPC-GOLD). Accordingly, CCGPMA-C proffers a more suitable representation of the labelers' behavior than its competitors. Indeed, CCGPMA-C codes both the annotators' dependencies and the relationship between the input features and the annotators' performance. To empirically support the above statement, Fig. 2 shows the estimated per-annotator reliability, where we only take into account models that include such types of parameters (MA-DGRL, CGPMA-C, and CCGPMA-C). As seen, MA-DGRL (see column 2 in Fig. 2) does not offer a proper representation of the annotators' behavior. CGPMA-C and CCGPMA-C (columns 3 and 4 in Fig. 2) outperforms MA-DGRL, which is a direct repercussion
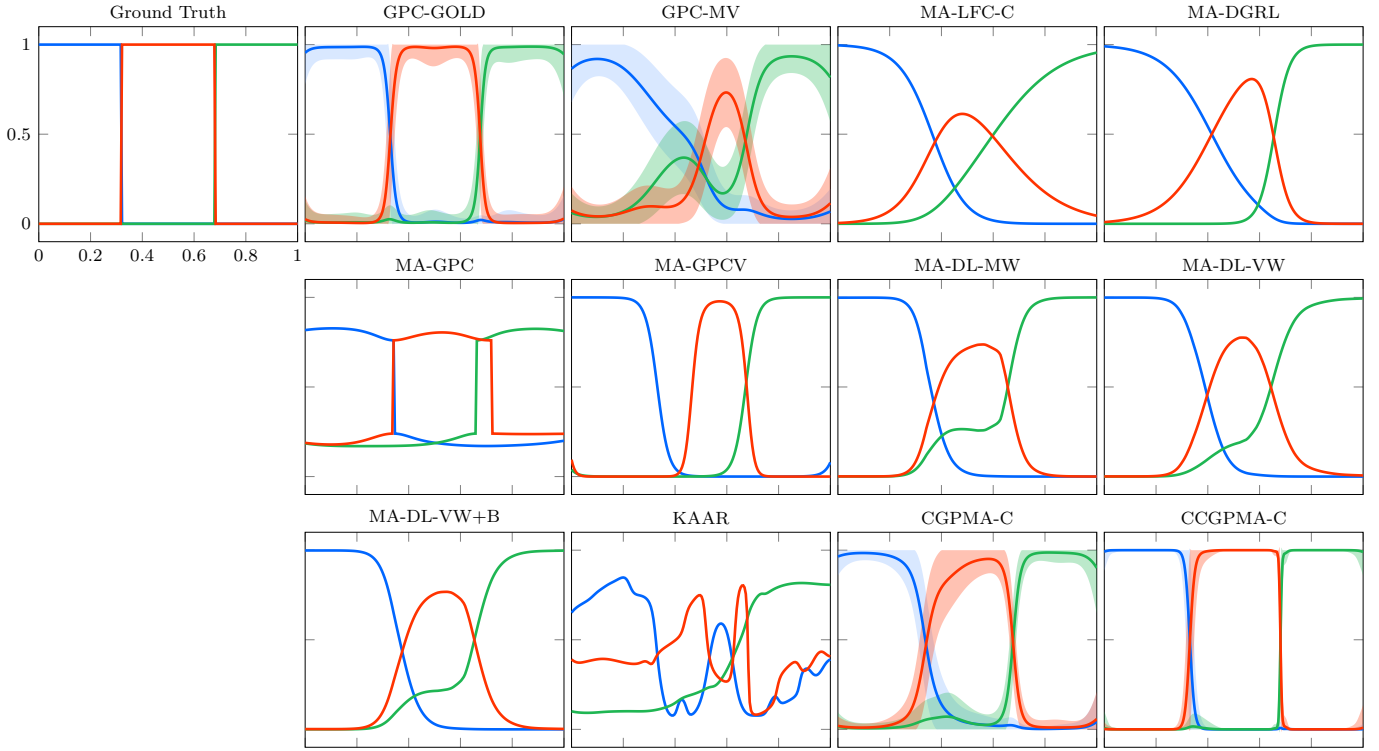
Fig. 1. Fully synthetic dataset results. The PLP is shown, comparing the prediction of our CCGPMA-C($AUC = 1$) and CCGPMA-C($AUC = 0.9999$) against: the theoretical upper bound GPC-GOLD($AUC = 1.0$), the lower bound GPC-MV($AUC = 0.9809$), and the state-of-the-art approaches MA-LFC-C($AUC = 0.9993$), MA-DGRL($AUC = 0.9999$), MA-GPC($AUC = 0.9977$), MA-GPCV($AUC = 0.9515$), MA-DL-MW($AUC = 0.9989$), MA-DL-VW($AUC = 0.9972$), MA-DL-VW+B($AUC = 0.9994$), KAAR(0.9099). Note that the shaded region in GPC-MV, CGPMA-C, and CCGPMA-C indicates the area enclosed by the mean $\pm$ two standard deviations. There is no shaded region for approaches lacking prediction uncertainty.

TABLE VI

AUC(%) CLASSIFICATION RESULTS FOR THE SEMI SYNTHETIC DATASETS. BOLD: THE HIGHEST AUC EXCLUDING THE UPPER BOUND (GPC-GOLD).

Method	Breast	Bupa	Ionosphere	Pima	TicTacToe	Occupancy	Skin	Western	Wine	Segmentation	Average
GPC-GOLD($M = 40$)	99.07 ± 0.45	69.75 ± 4.66	94.90 ± 2.35	83.78 ± 3.02	84.29 ± 3.34	99.56 ± 0.06	99.97 ± 0.01	91.85 ± 0.61	99.87 ± 0.15	95.96 ± 1.96	91.90
GPC-GOLD($M = 80$)	99.03 ± 0.46	69.97 ± 4.83	95.13 ± 2.25	83.74 ± 2.97	84.91 ± 3.23	99.56 ± 0.06	99.97 ± 0.01	92.50 ± 0.57	99.88 ± 0.16	97.81 ± 0.41	92.25
GPC-MV($M = 40$)	98.97 ± 0.45	53.66 ± 5.16	75.66 ± 5.72	53.99 ± 7.60	66.20 ± 3.57	75.85 ± 19.16	84.58 ± 0.90	86.58 ± 3.31	81.79 ± 2.12	95.62 ± 2.28	77.29
GPC-MV($M = 80$)	98.92 ± 0.48	56.98 ± 5.29	77.79 ± 5.50	53.02 ± 6.74	67.44 ± 3.57	63.12 ± 19.68	84.20 ± 0.80	84.46 ± 0.89	83.23 ± 4.87	97.49 ± 0.47	76.66
MA-LFC-C	87.89 ± 5.10	45.93 ± 14.44	73.58 ± 9.01	81.19 ± 3.13	60.04 ± 2.61	89.42 ± 0.79	$\mathbf{94.40 \pm 0.08}$	84.00 ± 2.11	96.92 ± 3.57	98.92 ± 0.31	81.23
MA-DGRL	97.57 ± 1.89	57.24 ± 3.36	64.53 ± 7.21	81.38 ± 2.90	61.29 ± 2.30	49.71 ± 1.05	93.79 ± 1.07	81.43 ± 1.50	97.95 ± 2.21	98.97 ± 0.38	78.39
MA-GPC	98.11 ± 1.16	54.46 ± 5.78	66.31 ± 14.74	53.25 ± 17.80	60.79 ± 9.95	92.57 ± 7.96	80.89 ± 0.60	86.71 ± 1.14	94.17 ± 2.62	97.34 ± 0.35	78.46
MA-GPCV	82.70 ± 5.47	55.67 ± 6.83	62.38 ± 8.71	62.17 ± 5.90	61.04 ± 10.03	64.09 ± 2.26	76.29 ± 3.74	84.51 ± 1.47	97.35 ± 1.72	99.24 ± 0.27	74.16
MA-DL-MW	94.70 ± 1.73	52.37 ± 5.68	75.35 ± 5.43	61.78 ± 2.67	68.27 ± 2.96	86.36 ± 0.57	90.92 ± 0.56	97.28 ± 1.09	99.50 ± 0.17	79.06
MA-DL-VW	95.26 ± 2.45	53.27 ± 6.18	69.87 ± 4.97	60.63 ± 3.36	67.71 ± 2.67	68.40 ± 3.45	86.56 ± 0.68	91.73 ± 0.67	98.07 ± 1.52	$\mathbf{99.72 \pm 0.11}$	79.12
MA-DL-VW+B	94.65 ± 2.42	52.81 ± 6.31	71.96 ± 4.53	61.23 ± 3.78	67.80 ± 3.42	67.82 ± 3.86	86.68 ± 0.67	91.64 ± 0.85	98.17 ± 1.55	$\mathbf{99.72 \pm 0.09}$	79.25
KAAR	80.58 ± 2.74	59.20 ± 6.63	70.46 ± 7.39	58.02 ± 4.06	63.81 ± 5.45	69.16 ± 2.06	51.58 ± 4.74	85.88 ± 1.20	99.43 ± 1.05	92.17 ± 1.90	73.03
CGPMA-C($M = 40$)	99.20 ± 0.38	57.13 ± 4.68	83.56 ± 10.02	82.01 ± 3.14	70.56 ± 3.04	82.20 ± 2.73	92.62 ± 1.20	91.78 ± 0.66	99.82 ± 0.18	96.79 ± 0.65	85.56
CGPMA-C($M = 80$)	99.14 ± 0.38	56.96 ± 4.74	86.15 ± 6.96	$\mathbf{82.04 \pm 3.18}$	70.48 ± 3.12	$\mathbf{99.08 \pm 0.26}$	90.46 ± 1.64	91.85 ± 0.57	$\mathbf{99.84 \pm 0.12}$	94.06 ± 0.61	87.01
CCGPMA-C($M = 40$)	$\mathbf{99.38 \pm 0.27}$	$\mathbf{60.22 \pm 5.06}$	87.84 ± 6.72	78.10 ± 6.22	$\mathbf{74.95 \pm 5.39}$	91.98 ± 2.00	85.70 ± 2.66	93.09 ± 0.51	99.44 ± 0.33	97.67 ± 0.53	86.84
CCGPMA-C($M = 80$)	99.33 ± 0.30	59.19 ± 5.65	$\mathbf{90.55 \pm 6.29}$	80.45 ± 5.10	73.12 ± 3.23	97.75 ± 2.00	89.42 ± 2.20	$\mathbf{93.15 \pm 0.50}$	99.43 ± 0.33	97.58 ± 0.43	$\mathbf{88.00}$

of modeling the labelers' parameters as functions of the input features. We observe that CCGPMA-C exhibits the best performance in terms of accuracy; such an outcome is due to this method improves the quality of the annotators' model by considering correlations among their decisions (26; 36)).

2) Semi-synthetic data results.: It is worth mentioning that the Semi-synthetic experiments are a common practice in the *learning from crowds* area (10; 36; 7), where the input features comes from real-world datasets whilst the labels from multiple annotators are simulated following the *fully synthetic data* set-up (see Eqs. (31) to (34)). Table VI shows the results concerning this second experiment. On average, our CCGPMA-C accomplishes the best predictive AUC; moreover,

we note that CGPMA-C reaches the second-best performance. Furthermore, the GPs-based competitors achieve competitive results (GPC-MV, MA-GPC, MA-GPCV, and KAAR). On the other hand, the GPC-MV method obtains a significantly lower performance than our CCGPMA-C, which is explained because GPC-MV is the most naive approach since it considers that the whole annotators exhibit the same performance. Conversely, analyzing the results from MA-GPC, MA-GPCV, and KAAR, we note that they perform worse than GPC-MV. We explain such an outcome in two ways. First, these approaches do not model the relationship between the input features and the annotators' performance. Second, as exposed in a previous experiment MA-GPC, MA-GPCV, and KAAR use a *one-*
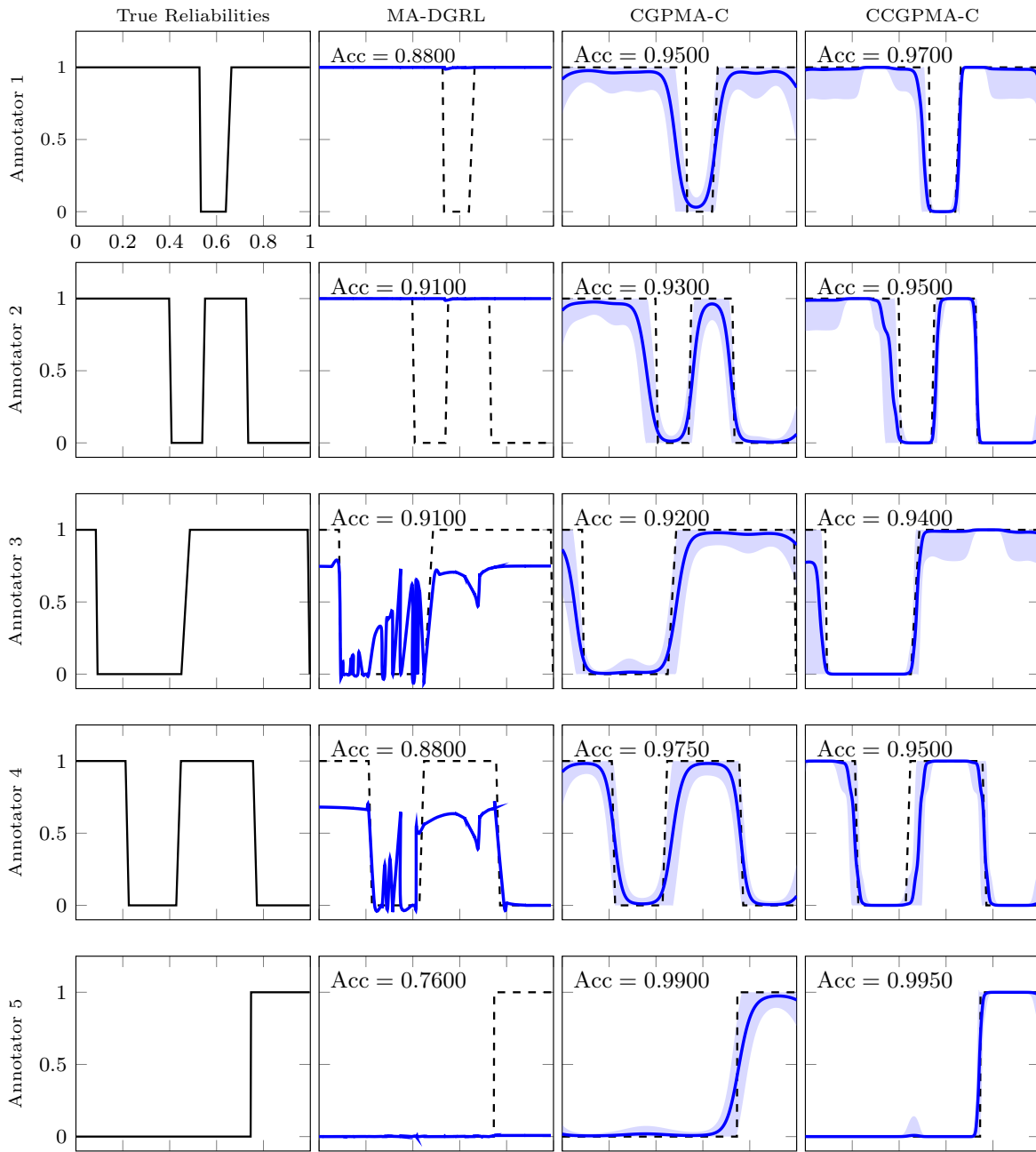
Fig. 2. Fully synthetic data reliability results. From top to bottom, the first column exposes the true reliabilities (λ_r). The subsequent columns present the estimation of the reliabilities performed by state-of-the-art models, where the correct values are provided in dashed lines. The shaded region in CGPMA-C and CCGPMA-C indicates the area enclosed by the mean $\pm$ two standard deviations. Also, the accuracy (Acc) is provided.

vs-all to deal with multi-class problems, which can lead to ambiguously classified regions (47). The latter can be confirmed in the results for the multi-class dataset "Western" ($K = 4$), where the predictive AUC for such approaches are the lowest. Then, analyzing the results from the DL-based strategies, we note a slightly better performance compared with the GPs-based methods (excluding CGPMA-C and CCGPMA-C). However, the DL-based performs considerably worse than our proposal because the CrowdLayer provides straightforward codification of the labelers' performance to guarantee a low computational cost (37). Finally, from the linear models, we

first analyze the outstanding performance from MA-DGRL, which defeats all its non-linear competitors. In particular, the simulated labels (see Section IV-A1) follows the MA-DGRL model, favoring its performance. Though MA-LFC-C achieves competitive performance compared to the DL-based methods, it is considerably lower than our proposal. In fact, the MA-LFC-C formulation assumes that the annotators' behavior is homogeneous across the input space, which does not correspond to the labels simulation procedure.

3) Fully real data results.: We test the *fully real datasets*, which configure the most challenging scenario. The input

features and the labels from multiple experts come from real-world applications. Table VII outlines the achieved AUC. First, we observe that for the voice data, G and R scales exhibit a similar AUC for all considered approaches; in fact, GPC-MV obtains a result comparable with the upper bound GPC-GOLD. The latter can be explained in the sense that the annotators exhibit a suitable performance for these scales, i.e., the provided labels are similar to the ground truth. On the other hand, a reduction in the predictive AUC is observed for scale B, which is a consequence of diminishing the labelers' performance compared with scales G and R, as demonstrated in (13). Our approaches exhibit the best generalization performances for the three scales in the voice dataset. Remarkably, CGPMA-C and CCGPMA-C do not suffer significant changes in the scale B, which is an outstanding outcome because it reflects that our method offers a better representation of the labelers' behavior against low-quality annotations. Finally, we review the AUC for the Music dataset. Achieved results show a low performance for the MA-GPC, even lower than their intuitive lower bound (GPC-MV). Notably, our CCGPMA-C reaches the best predictive AUC, being comparable with the intuitive upper bound.

TABLE VII
AUC CLASSIFICATION RESULTS FOR THE FULLY REAL DATASETS. BOLD: THE HIGHEST PERFORMANCE EXCLUDING THE GPC-GOLD BOUND.

Method	Voice			Music	Average
	G	R	B		
GPC-GOLD($M = 40$)	0.9481	0.9481	0.9481	0.9358	0.9450
GPC-GOLD($M = 80$)	0.9484	0.9484	0.9484	0.9178	0.9407
GPC-MV($M = 40$)	0.8942	0.9373	0.8001	0.8871	0.8797
GPC-MV($M = 80$)	0.9301	0.9377	0.7962	0.8897	0.8884
MA-LFC-C	0.9122	0.9130	0.8406	0.8599	0.8814
MA-DGRL	0.9127	0.9164	0.8259	0.8832	0.8845
MA-GPC	0.8660	0.8597	0.4489	0.8253	0.7500
MA-GPCV	0.9283	0.9208	0.8835	0.8677	0.9001
MA-DL-MW	0.8957	0.8966	0.8123	0.8567	0.8653
MA-DL-VW	0.8942	0.8929	0.8092	0.9167	0.8782
MA-DL-VW+B	0.9030	0.8937	0.8218	0.8573	0.8689
KAAR	0.9109	0.9351	0.8969	0.8896	0.9081
CGPMA-C($M = 40$)	**0.9324**	0.9406	0.8696	0.9025	0.9113
CGPMA-C($M = 80$)	**0.9324**	0.9417	0.8708	0.8987	0.9109
CCGPMA-C($M = 40$)	0.9318	**0.9422**	**0.9002**	0.9446	**0.9297**
CCGPMA-C($M = 80$)	0.9243	0.9383	0.8907	**0.9456**	0.9247

B. Regression

1) Fully synthetic data results : We perform a controlled experiment aiming to verify the capability of our CGPMA and CCGPMA to estimate the performance of inconsistent annotators as a function of the input space and taking into account their dependencies. For this first experiment, we use the *fully synthetic* dataset described in Section IV-B1. We simulate five labelers ($R = 5$) with different levels of expertise. To simulate the error-variances, we define $Q = 3$ functions $\hat{\mu}_q(\cdot)$, which are given as

$$\hat{\mu}_1(x) = 4.5\cos(2\pi x + 1.5\pi) - 3\sin(4.3\pi x + 0.3\pi) + \cdots$$
$$\cdots + 4\cos(7\pi x + 2.4\pi), \quad (35)$$
$$\hat{\mu}_2(x) = 4.5\cos(1.5\pi x + 0.5\pi) + 5\sin(3\pi x + 1.5\pi) - \cdots$$
$$- 4.5\cos(8\pi x + 0.25\pi), \quad (36)$$
$$\hat{\mu}_3(x) = 1, \quad (37)$$

where $x \in [0, 1]$. Besides, we define the following combination matrix $\hat{W} \in \mathbb{R}^{Q \times R}$, where

$$\hat{W} = \begin{bmatrix} -0.10 & 0.01 & -0.05 & 0.01 & -0.01 \\ 0.10 & -0.01 & 0.01 & -0.05 & 0.05 \\ -2.3 & -1.77 & 0.54 & 0.9 & 1.42 \end{bmatrix}, \quad (38)$$

holding elements $w_{l_r,q}$.

Fig. 3 shows the predictive performance of all methods in this first experiment. The results show two clear groups: those based on GPs (GPR-Av, MA-GPR, CGPMA-R, and CCGPMA-R), which expose the best performance in terms of the R^2 score, and those based on other types of approaches (MA-LFCR, and MA-DL), whose performance is not satisfactory. The behavior of MA-LFCR is low since it only can deal with linear problems. Besides, concerning MA-DL and its three variations (S, B, and S+B), we note that this approach can deal with non-linear dynamics. However, MA-DL reaches a significantly low performance (even lower than the most naive approach, GPR-Av). To explain such an outcome, we remark that MA-DL comprises the introduction of an additional layer, the "CrowdLayer", which allows the training of neural networks directly from the noisy labels of multiple annotators (18). Yet, such a CrowdLayer provides a very simple codification of the annotators' performance to guarantee a low computational cost (37); therefore, MA-DL does not provide a proper codification of the annotators' behavior. On the other hand, among the GP-based methods, the proposed CCGPMA-R achieves the best performance in terms of R^2, followed closely by CGPMA-R and MA-GPR.

Besides, concerning the high performance of our CCGPMA-R (the best in terms of R^2 score), we hypothesize that such an outcome is a consequence of our method offers a better representation of the labelers' behavior when compared with its competitors. To empirically support the above hypothesis, Fig. 4 shows the estimated error-variances for this first experiment; here, we only take into account the models that include these parameters in their formulations. As seen in Fig. 4, MA-LFCR and MA-GPR offer the worst representation for the annotator's performance, which is due to such methods do not take into account the relationship between the annotators and the input space. Conversely, CGPMA-R and CCGPMA-R outperform the models named previously. This outcome is a consequence that such two approaches compute the error-variance as a function of the input features, allowing for a better codification of the labelers' behavior. Besides, by making a visual inspection and analyzing the R^2 scores, CCGPMA-R performs better than CGPMA-R because the former codes properly the annotators' interdependencies (26). Finally, we remark that although our CCGPMA-R achieves the best representation of the annotators' performance, Annotator 4 exhibits a lower performance in terms of R^2 score compared with the other labelers. Such an outcome is caused by the quasi-periodic behavior in the error-variances for those labelers, which cannot be captured because we are using an RBF-based kernel.

2) Results over semi-synthetic data: Table VIII shows the results of the *semi synthetic datasets*. On average, our CCGPMA-R exhibits the best generalization performance in
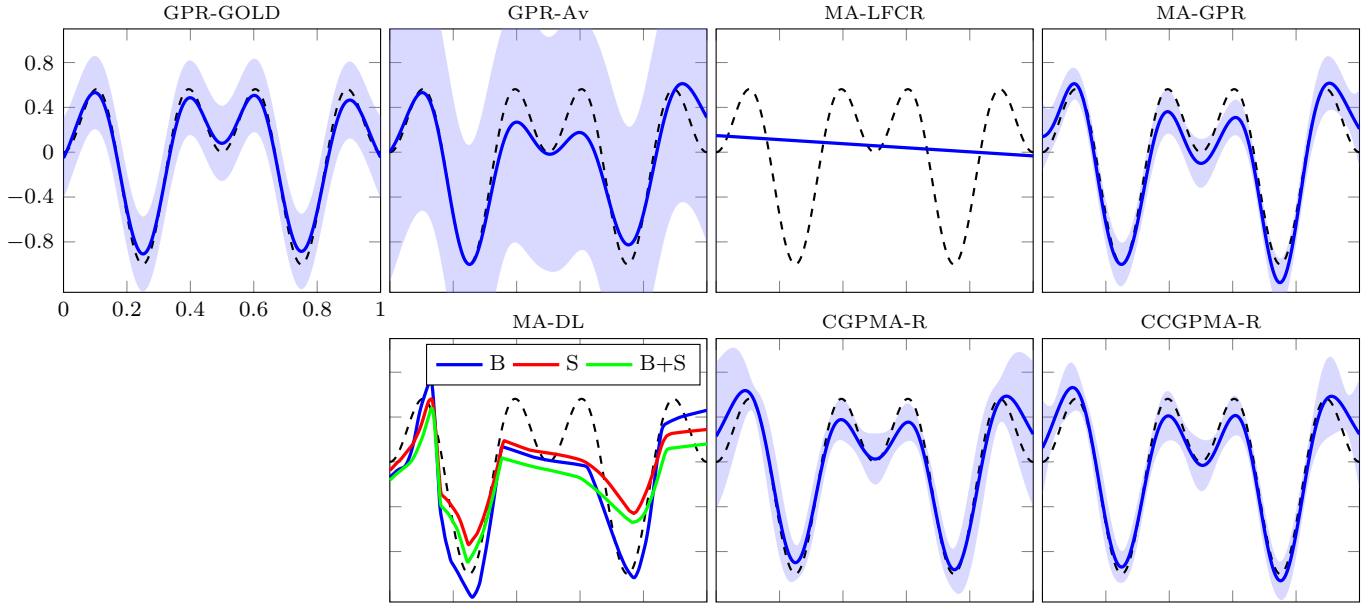
Fig. 3. Fully synthetic dataset results. We compare the prediction of our CCGPMA-R($R^2 = 0.9438$), and CGPMA-R($R^2 = 0.9280$) with the theoretical upper bound GPR-GOLD($R^2 = 0.9843$) and lower bound GPR-Av($R^2 = 0.8718$), and state-of-the-art approaches, MA-LFCR($R^2 = -0.0245$), MA-GPR($R^2 = 0.9208$), MA-DL-B($R^2 = 0.7020$), MA-DL-S($R^2 = 0.6559$), MA-DL-B+S($R^2 = 0.5997$). Note that we provided the Gold Standard in dashed lines. The shaded region in GPR-Av, MA-GPR, CGPMA-R, and CCGPMA-R indicates the area enclosed by the mean plus or minus two standard deviations. We remark that there is no shaded region for MA-LFCR, and DLMA since they do not provide information about the prediction uncertainty.

terms of the R^2 score. On the other hand, regarding its GP-based competitors (GPR-Av, MA-GPR, and CGPMA-R), we first note that the performance of CGPMA-R exhibits a similar (but lower) performance than CCGPMA-R. The above is a consequence of that conversely to CGPMA-R, our CCGPMA-R models the annotators' interdependencies. Secondly, the intuitive lower bound GPR-Av exhibits a significantly worse prediction than our approaches. We remark on MA-GPR's behavior, which is lowest compared with its GPs-based competitors, even far worse than the supposed lower bound GPR-Av. The key to this abnormal outcome lies in the formulation of this approach; MA-GPR models the annotators' behavior by assuming that their performance does not depend on the input features and considering that the labelers make their decisions independently, which does fit the process that we use to simulate the labels.

Next, we analyze the results concerning the linear model MA-LFR; attained to the results, we note that this approach's prediction capacity is far lower than ours. The above outcome suggests that there may exist a non-linear structure in most databases. However, we highlight a particular result for the dataset CT, where MA-LFCR exhibits the best performance defeating all its competitors based on non-linear models. From the above, we intuit that the CT dataset may have a linear structure. To confirm this supposition, we perform an additional experiment over CT by training a regression scheme based on LR with the actual labels (we follow the same scheme as for GPR-GOLD). We obtain an R^2 score equal to 0.8541 (on average), which is close to GPR-GOLD results. Thus, we can elucidate that there exists a linear structure in the dataset CT. Finally, we analyze the results for the DL-based models. Similar to the experiments over *fully synthetic datasets*, we note a considerable low prediction capacity; in fact, they are even defeated by the linear model MA-LFR. Again, we attribute

TABLE VIII
REGRESSION RESULTS IN TERMS OF R^2 SCORE OVER *semi synthetic datasets*. BOLD: THE HIGHEST R^2 EXCLUDING THE UPPER BOUND GPR-GOLD.

| Method	Auto	Bike	Concrete	Housing	Yacht	CT	Average
GPR-GOLD($M = 40$)	0.8604 ± 0.0271	0.5529 ± 0.0065	0.8037 ± 0.0254	0.8235 ± 0.0419	0.8354 ± 0.0412	0.8569 ± 0.0055	0.7888
GPR-GOLD($M = 80$)	0.8612 ± 0.0279	0.5603 ± 0.0063	0.8271 ± 0.0230	0.8275 ± 0.0399	0.8240 ± 0.0339	0.8648 ± 0.0047	0.7942
GPR-Av($M = 40$)	0.8425 ± 0.0286	0.5280 ± 0.0100	0.7589 ± 0.0279	0.7834 ± 0.0463	0.7588 ± 0.0498	0.8070 ± 0.0130	0.7464
GPR-Av($M = 80$)	0.8406 ± 0.0304	0.5397 ± 0.0085	0.7765 ± 0.0274	0.7903 ± 0.0451	0.7676 ± 0.0535	0.8167 ± 0.0089	0.7552
MA-LFCR	0.7973 ± 0.0218	0.3385 ± 0.0051	0.6064 ± 0.0384	0.7122 ± 0.0509	0.6403 ± 0.0186	0.8400 ± 0.0014	0.6558
MA-GPR	0.8456 ± 0.0281	0.4448 ± 0.0187	0.7769 ± 0.0367	0.7685 ± 0.0632	0.7842 ± 0.1027	0.0105 ± 0.0045	0.6051
MA-DL-B	0.7766 ± 0.0253	$\mathbf{0.5854 \pm 0.0107}$	0.2319 ± 0.0328	0.5317 ± 0.1005	0.2089 ± 0.0783	$\mathbf{0.6903 \pm 0.2689}$	0.5041
MA-DL-S	0.7761 ± 0.0279	0.5828 ± 0.0149	0.2363 ± 0.0252	0.5352 ± 0.0948	0.1822 ± 0.0985	$\mathbf{0.8418 \pm 0.2288}$	0.5257
MA-DL-B+S	0.7717 ± 0.0239	0.5816 ± 0.0181	0.2369 ± 0.0322	0.5330 ± 0.0850	0.1974 ± 0.0895	0.5517 ± 0.2316	0.4787
CGPMA-R($M = 40$)	0.8476 ± 0.0229	0.5464 ± 0.0069	0.8169 ± 0.0231	0.7244 ± 0.2973	0.8049 ± 0.0482	0.8236 ± 0.0132	0.7606
CGPMA-R($M = 80$)	0.8342 ± 0.0217	0.5560 ± 0.0074	0.8190 ± 0.0254	0.7259 ± 0.3018	0.7928 ± 0.0884	0.8371 ± 0.0104	0.7608
CCGPMA-R($M = 40$)	$\mathbf{0.8558 \pm 0.0248}$	0.5284 ± 0.0117	0.7976 ± 0.0270	0.8169 ± 0.0468	0.8409 ± 0.0548	0.8219 ± 0.0062	0.7769
CCGPMA-R($M = 80$)	0.8534 ± 0.0243	0.5467 ± 0.0069	$\mathbf{0.8220 \pm 0.0259}$	$\mathbf{0.8215 \pm 0.0466}$	$\mathbf{0.8691 \pm 0.0473}$	0.8252 ± 0.0083	$\mathbf{0.7897}$
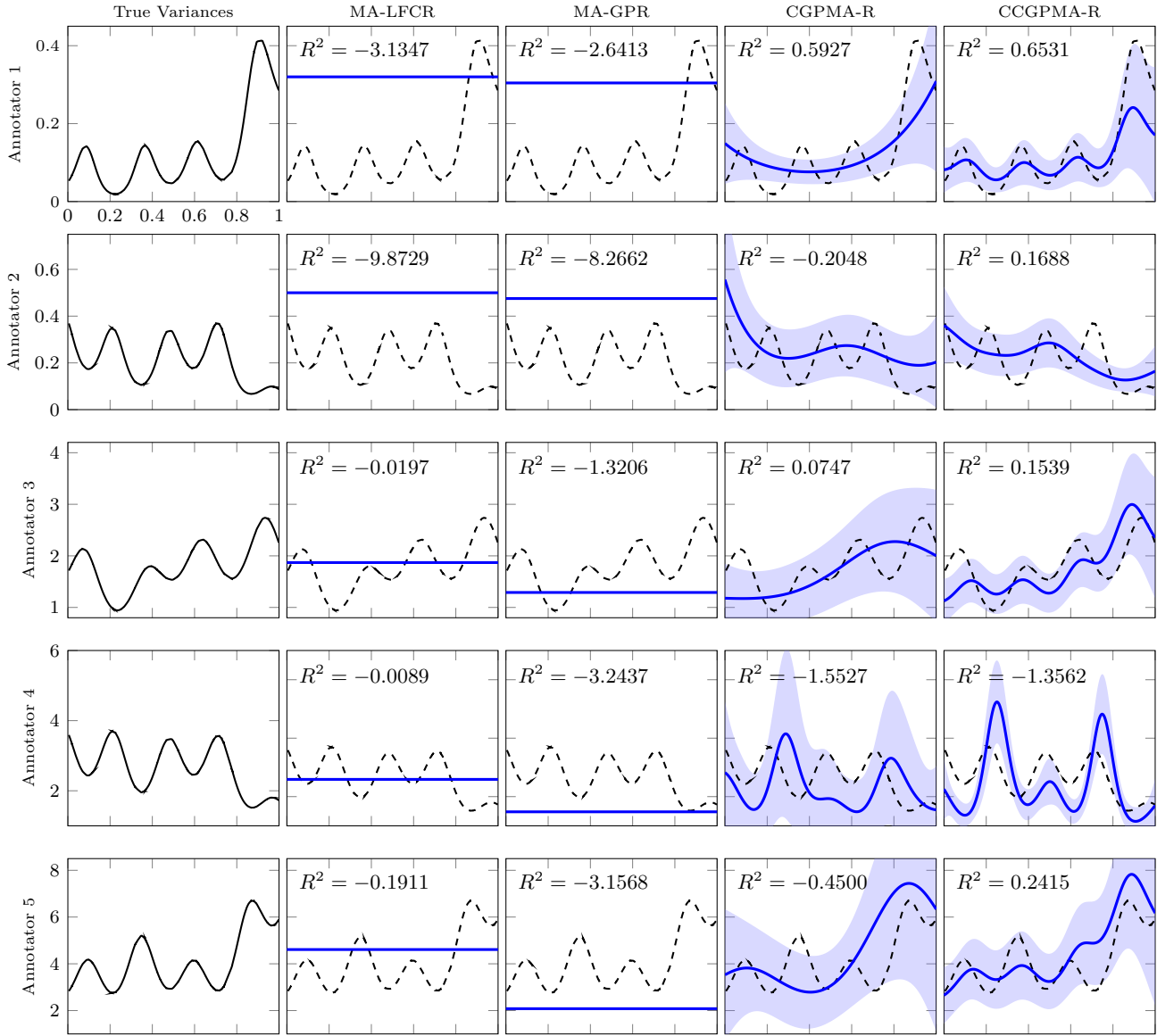
Fig. 4. Estimated values of error-variance for the five annotators in the *fully synthetic* experiment. In the first column, from top to bottom, we expose the error-variances used to simulate the labels from each annotator. Furthermore, the subsequent columns from top to bottom present the estimation of such error-variances performed by state-of-the-art models that include these kinds of parameters in their formulation; moreover, the true error-variances are provided in dashed lines. The shaded region in CGPMA-R and CCGPMA-R indicates the area enclosed by the mean plus or minus two standard deviations. We remark that there is no shaded region for MA-LFCR, and MA-GPR since these approaches perform a fixed-point estimation for the annotators' parameters. Finally, we remark that the R^2 score between the true and estimated error variances are provided.

this behavior to the fact that the CrowdLayer (used to manage the data from multiple annotators) does not offer a suitable codification of the labelers' behavior. Nevertheless, taking the above into account, we observe a remarkable result in the Bike dataset. The DL-based approaches offer the best performance, even defeating the supposed upper-bound GPR-GOLD. To explain that, it is necessary to analyze the meaning of the target variable in such a dataset. Regarding the description of this dataset,[6] the target variables indicate the count of total rental bikes, including both casual and registered in a day. The above suggests that there may exist a quasi-periodic structure in the dataset, which the GPR-GOLD cannot capture since it

uses a non-periodic kernel (RBF). To support our suppositions, an additional experiment was performed over this dataset by training the model GPR-GOLD with the following kernel:

$$\kappa(\boldsymbol{x}_n, \boldsymbol{x}_{n'}) = \varphi \exp\left[-\frac{1}{2}\sum_{p=1}^{P}\left(\frac{\sin\left(\frac{\pi(x_{p,n}-x_{p,n'})}{T_p}\right)}{l_p}\right)^2\right], \quad (39)$$

where $\varphi \in \mathbb{R}$ is the variance parameter, $l_p \in (\mathbb{R}^+)$ is the length-scale parameter for the p-th dimension, and $T_p \in (\mathbb{R}^+)$ is the period for the p-th dimension. Therefore, we obtain an R^2 score equal to 0.5952 (on average), which is greater than

---

[6] https://archive.ics.uci.edu/ml/datasets/bike+sharing+dataset

the obtained by the DL-based approaches, indicating a quasi-periodic structure in the Bike dataset as we had supposed.

3) Fully real data results: Finally, we use the *fully real datasets*, which present the most challenging scenario, where both the input samples and the labels come from real-world applications. Table IX outlines the achieved performances. We

TABLE IX
REGRESSION RESULTS IN TERMS OF R^2 SCORE OVER *fully real dataset*.
BOLD: THE HIGHEST R^2 EXCLUDING THE UPPER BOUND GPR-GOLD.

Method	Music
GPR-GOLD($M = 40$)	0.4704
GPR-GOLD($M = 80$)	0.4889
GPR-Av($M = 40$)	0.2572
GPR-Av($M = 80$)	0.2744
MA-LFCR	0.1404
MA-GPR	0.0090
MA-DL-B	0.2339
MA-DL-S	0.2934
MA-DL-B+S	0.3519
CGPMA-R($M = 40$)	0.3345
CGPMA-R($M = 80$)	0.3531
CCGPMA-R($M = 40$)	0.3337
CCGPMA-R($M = 80$)	**0.3872**

remark that our CCGPMA-R with $M = 80$ obtains the best generalization performance in terms of the R^2 score. Further, as theoretically expected, its performance lies between that of GPR-GOLD and GP-Av. Moreover, regarding the GP-based competitors (MA-GPR and CGPMA-R), we note that our CGPMA-R is just a bit lower than CCGPMA-R. On the other hand, MA-GPR exhibits the worst prediction capability with a R^2 close to zero. We suppose the above is a symptom of overfitting, which can be confirmed because the training R^2 score for MA-GPR is 0.4731, comparable with GPR-GOLD. Conversely, the linear approach MA-LFCR exhibits the second-lowest performance and performs worse than the theoretical lower bound GP-Av, which indicates a non-linear structure in the Music dataset. Finally, analyzing the results from the deep learning approaches, we note that the variation MA-DL-B+S exhibits a similar performance compared with our CGPMA-R; however, it is slightly lower than our CCGPMA-R. We highlight that despite deep learning capacities, our approach CCGPMA-R offers a better representation of annotators' behavior, unlike the deep learning techniques, which measure such performance using a single parameter.

Also, we observe that all regression models presented a lower generalization performance than previous results (see Table V in the paper) over the same dataset. The above is a repercussion of solving a multi-class classification problem with regression models. Such an outcome is not uncommon, and it can be founded in works (18; 15).

VI. CONCLUSION

This paper introduces a novel Gaussian Process-based approach to deal with Multiple Annotators scenarios, termed Correlated Chain Gaussian Process for Multiple Annotators (CCGPMA). Our method is built as an extension of the chained GP (27), introducing a semi-parametric latent factor model (SLFM) to exploit correlations between the GP latent functions that model the parameters of a given likelihood function. To the

best of our knowledge, CCGPMA is the first attempt to build a probabilistic framework that codes the annotators' expertise as a function of the input data and exploits the correlations among the labelers' answers. Besides, we highlight that our approach can be used with different likelihood, which allows us to deal with both categorical data (classification) and real-valued (regression). We tested our approach for classification tasks using different scenarios concerning the provided annotations: synthetic, semi-synthetic, real-world experts. According to the results, we remark that our CCGPMA can achieve robust predictive properties for the studied datasets, outperforming state-of-the-art methods.

As future work, CCGPMA can be extended by using convolution processes (48) instead of the SLFM, aiming to obtain a better representation of the correlations among the labelers. Also, our approach can be extended for multi-task learning in the context of multiple annotators (49). Finally, we note that the performance of our approach heavily depend on kernel selection (see Section V-B2); accordingly, it would be interesting to automatically perform such kernel selection (50) as an input block of our framework.

REFERENCES

[1] J. Zhang, V. S. Sheng, and J. Wu, "Crowdsourced label aggregation using bilayer collaborative clustering," *IEEE Transactions on Neural Networks and Learning Systems*, vol. 30, no. 10, pp. 3172–3185, 2019.

[2] Y. Liu, W. Zhang, Y. Yu *et al.*, "Truth inference with a deep clustering-based aggregation model," *IEEE Access*, vol. 8, pp. 16 662–16 675, 2020.

[3] Y. Kara, G. Genc, O. Aran, and L. Akarun, "Modeling annotator behaviors for crowd labeling," *Neurocomputing*, vol. 160, pp. 141–156, 2015.

[4] R. Snow, B. O'Connor, D. Jurafsky, and A. Ng, "Cheap and fast—but is it good?: evaluating non-expert annotations for natural language tasks," in *EMNLP*. ACL, 2008, pp. 254–263.

[5] D. Tao, J. Cheng, Z. Yu, K. Yue, and L. Wang, "Domain-weighted majority voting for crowdsourcing," *IEEE transactions on neural networks and learning systems*, vol. 30, no. 1, pp. 163–174, 2018.

[6] G. Rizos and B. W. Schuller, "Average jane, where art thou?–recent avenues in efficient machine learning under subjectivity uncertainty," in *International Conference on Information Processing and Management of Uncertainty in Knowledge-Based Systems*. Springer, 2020, pp. 42–55.

[7] P. Morales-Álvarez, P. Ruiz, S. Coughlin, R. Molina, and A. K. Katsaggelos, "Scalable variational Gaussian processes for crowdsourcing: Glitch detection in LIGO," *arXiv preprint arXiv:1911.01915*, 2019.

[8] J. Zhang, X. Wu, and V. S. Sheng, "Imbalanced multiple noisy labeling," *IEEE Transactions on Knowledge and Data Engineering*, vol. 27, no. 2, pp. 489–503, 2014.

[9] A. Dawid and A. Skene, "Maximum likelihood estimation of observer error-rates using the EM algorithm," *Appl. Stat.*, pp. 20–28, 1979.

[10] P. Ruiz, P. Morales-Álvarez, R. Molina, and A. K. Katsaggelos, "Learning from crowds with variational Gaussian processes," *Pattern Recognition*, vol. 88, pp. 298–311, 2019.

[11] V. C. Raykar, S. Yu, L. H. Zhao, G. H. Valadez, C. Florin, L. Bogoni, and L. Moy, "Learning from crowds," *J. Speech Lang. Hear. Res.*, vol. 11, no. Apr, pp. 1297–1322, 2010.

[12] F. Rodrigues, F. C. Pereira, and B. Ribeiro, "Gaussian process classification and active learning with multiple annotators." in *ICML*, 2014, pp. 433–441.

[13] J. Gil, M. Álvarez, and Á. Orozco, "Automatic assessment of voice quality in the context of multiple annotations," in *EMBC*. IEEE, 2016, pp. 6236–6239.

[14] P. Groot, A. Birlutiu, and T. Heskes, "Learning from multiple annotators with Gaussian processes," in *ICANN*. Springer, 2011, pp. 159–164.

[15] F. Rodrigues, M. Lourenco, B. Ribeiro, and F. Pereira, "Learning supervised topic models for classification and regression from crowds," *IEEE transactions on PAMI*, 2017.

[16] F. Rodrigues, F. Pereira, and B. Ribeiro, "Sequence labeling with multiple annotators," *Machine learning*, vol. 95, no. 2, pp. 165–181, 2014.

[17] S. Albarqouni, C. Baur, F. Achilles, V. Belagiannis, S. Demirci, and N. Navab, "Aggnet: deep learning from crowds for mitosis detection in breast cancer histology images," *IEEE transactions on medical imaging*, vol. 35, no. 5, pp. 1313–1321, 2016.

[18] F. Rodrigues and F. C. Pereira, "Deep learning from crowds," in *Thirty-Second AAAI Conference on Artificial Intelligence*, 2018.

[19] M. Y. Guan, V. Gulshan, A. M. Dai, and G. E. Hinton, "Who said what: Modeling individual labelers improves classification," in *Thirty-Second AAAI Conference on Artificial Intelligence*, 2018.

[20] E. Rodrigo, J. Aledo, and J. Gámez, "Machine learning from crowds: A systematic review of its applications," *Wiley Interdisciplinary Reviews: Data Mining and Knowledge Discovery*, vol. 9, no. 2, p. e1288, 2019.

[21] M. Venanzi, J. Guiver, G. Kazai, P. Kohli, and M. Shokouhi, "Community-based bayesian aggregation models for crowdsourcing," in *Proceedings of the 23rd international conference on World wide web*. ACM, 2014, pp. 155–164.

[22] W. Tang, M. Yin, and C.-J. Ho, "Leveraging peer communication to enhance crowdsourcing," in *The World Wide Web Conference*. ACM, 2019, pp. 1794–1805.

[23] P. Zhang and Z. Obradovic, "Learning from inconsistent and unreliable annotators by a Gaussian mixture model and Bayesian information criterion," in *Joint European Conference on Machine Learning and Knowledge Discovery in Databases*. Springer, 2011, pp. 553–568.

[24] J. Surowiecki, *The wisdom of crowds*. Anchor, 2005.

[25] U. Hahn, M. von Sydow, and C. Merdes, "How communication can make voters choose less well," *Topics in cognitive science*, 2018.

[26] T. Zhu, M. A. Pimentel, G. D. Clifford, and D. A. Clifton, "Unsupervised bayesian inference to fuse biosignal sensory estimates for personalising care," *IEEE J. BIOMED. HEALTH*, vol. 23, no. 1, p. 47, 2019.

[27] A. Saul, J. Hensman, A. Vehtari, and N. Lawrence, "Chained Gaussian processes," in *Artificial Intelligence and Statistics*, 2016, pp. 1431–1440.

[28] M. A. Álvarez, L. Rosasco, N. D. Lawrence *et al.*, "Kernels for Vector-Valued functions: A review," *Foundations and Trends® in Machine Learning*, vol. 4, no. 3, pp. 195–266, 2012.

[29] Y. Teh, M. Seeger, and M. Jordan, "Semiparametric latent factor models," in *AISTATS 2005-Proceedings of the 10th International Workshop on Artificial Intelligence and Statistics*, 2005.

[30] M. Álvarez, D. Luengo, M. Titsias, and N. D. Lawrence, "Efficient multioutput Gaussian processes through variational inducing kernels," in *Proceedings of the Thirteenth International Conference on Artificial Intelligence and Statistics*, 2010, pp. 25–32.

[31] M. D. Hoffman, D. M. Blei, C. Wang, and J. Paisley, "Stochastic variational inference," *The Journal of Machine Learning Research*, vol. 14, no. 1, pp. 1303–1347, 2013.

[32] F. Rodrigues, F. Pereira, and B. Ribeiro, "Learning from multiple annotators: Distinguishing good from random labelers," *Pattern Recognition Letters*, vol. 34, no. 12, pp. 1428–1436, 2013.

[33] Y. Yan, R. Rosales, G. Fung, R. Subramanian, and J. Dy, "Learning from multiple annotators with varying expertise," *Machine learning*, vol. 95, no. 3, pp. 291–327, 2014.

[34] X. Wang and J. Bi, "Bi-convex optimization to learn classifiers from multiple biomedical annotations," *IEEE/ACM transactions on computational biology and bioinformatics*, vol. 14, no. 3, pp. 564–575, 2016.

[35] H. Xiao, H. Xiao, and C. Eckert, "Learning from multiple observers with unknown expertise," in *Pacific-Asia Conference on Knowledge Discovery and Data Mining*. Springer, 2013, pp. 595–606.

[36] J. Gil-Gonzalez, A. Alvarez-Meza, and A. Orozco-Gutierrez, "Learning from multiple annotators using kernel alignment," *Pattern Recognition Letters*, vol. 116, pp. 150–156, 2018.

[37] P. Morales-Álvarez, P. Ruiz, R. Santos-Rodríguez, R. Molina, and A. K. Katsaggelos, "Scalable and efficient learning from crowds with Gaussian processes," *Information Fusion*, vol. 52, pp. 110–127, 2019.

[38] G. Hua, C. Long, M. Yang, and Y. Gao, "Collaborative active visual recognition from crowds: A distributed ensemble approach," *IEEE transactions on pattern analysis and machine intelligence*, vol. 40, no. 3, pp. 582–594, 2018.

[39] C. E. Rasmussen and C. K. Williams, *Gaussian processes for machine learning*. MIT press Cambridge, 2006, vol. 1.

[40] J. Hensman, A. G. Matthews, and Z. Ghahramani, "Scalable variational Gaussian process classification," *Proceedings of Machine Learning Research*, vol. 38, pp. 351–360, 2015.

[41] P. Moreno-Muñoz, A. Artés, and M. Alvarez, "Heterogeneous multi-output Gaussian process prediction," in *Advances in neural information processing systems*, 2018, pp. 6711–6720.

[42] D. M. Blei, A. Kucukelbir, and J. D. McAuliffe, "Variational inference: A review for statisticians," *Journal of the American statistical Association*, vol. 112, no. 518, pp. 859–877, 2017.

[43] J. A. Hernández-Muriel, J. B. Bermeo-Ulloa, M. Holguin-Londoño, A. M. Álvarez-Meza, and Á. A. Orozco-Gutiérrez, "Bearing health monitoring using relief-f-based feature relevance analysis and HMM," *Applied Sciences*, vol. 10, no. 15, p. 5170, 2020.

[44] J. Arias, J. Godino, J. Gutiérrez, V. Osma, and N. Sáenz, "Automatic GRBAS assessment using complexity measures and a multiclass GMM-based detector," *Models and Analysis of Vocal Emissions for Biomedical Applications*, pp. 111–114, 2011.

[45] L. v. d. Maaten and G. Hinton, "Visualizing data using t-SNE," *Journal of machine learning research*, vol. 9, no. Nov, pp. 2579–2605, 2008.

[46] T. Fawcett, "An introduction to ROC analysis," *Pattern recognition letters*, vol. 27, no. 8, pp. 861–874, 2006.

[47] C. Bishop, *Pattern recognition and machine learning*. springer, 2006.

[48] M. A. Álvarez and N. D. Lawrence, "Computationally efficient convolved multiple output Gaussian processes," *The Journal of Machine Learning Research*, vol. 12, pp. 1459–1500, 2011.

[49] M. A. Alvarez, L. Rosasco, and N. D. Lawrence, "Kernels for vector-valued functions: A review," *arXiv preprint arXiv:1106.6251*, 2011.

[50] A. B. Abdessalem, N. Dervilis, D. J. Wagg, and K. Worden, "Automatic kernel selection for gaussian processes regression with approximate bayesian computation and sequential monte carlo," *Frontiers in Built Environment*, vol. 3, p. 52, 2017.

J. Gil-Gonzalez received his undergraduate degree in electronic engineering (2014) from the Universidad Tecnológica de Pereira, Colombia. His M.Sc. in electrical engineering (2016) from the same university. Currently, he is PhD student from the same university. His research interests include probabilistic models for machine learning, learning from crowds, and Bayesian inference.

Juan-José Giraldo Received a degree in Electronics Engineering (B. Eng.) with Honours, from Universidad del Quindío, Colombia in 2009, a master degree in Electrical Engineering (M. Eng.) from Universidad Tecnológica de Pereira, Colombia in 2015. Currently, Mr. Giraldo is a Ph.D student in Comp. Science at the University of Sheffield, UK

A.M. Álvarez-Meza received his undergraduate degree in electronic engineering (2009), his M.Sc. degree in engineering (2011), and his Ph.D. in automatics from the Universidad Nacional de Colombia. He is a Professor in the Department of Electrical, Electronic and Computation Engineering at the Universidad Nacional de Colombia - Manizales. His research interests include machine learning and signal processing.

A. Orozco-Gutierrez received his undergraduate degree in electrical engineering (1985) and his M.Sc. degree in electrical engineering (2004) from Universidad Tecnológica de Pereira, and his Ph.D. in bioengineering (2009) from Universidad Politecnica de Valencia (Spain). He received his undergraduate degree in law (1996) from Universidad Libre de Colombia. He is a Professor in the Department of Electrical Engineering at the Universidad Tecnologica de Pereira. His research interests include bioengineering.

M. A. Álvarez received the BEng degree in electronics engineering from the Universidad Nacional de Colombia (2004), the M.Sc. degree in electrical engineering from the Universidad Tecnologica de Pereira, Colombia (2006), and the PhD degree in computer science from The University of Manchester, UK (2011). Currently, he is a Lecturer of Machine Learning in the Department of Computer Science, University of Sheffield, United Kingdom. His research interests include probabilistic models, kernel methods, and stochastic processes.